A COMPARISON BETWEEN MODEL AND FIELD DIESEL MASS RECOVERY IN DOLOMITE KARST

By

CULLEN MIKAEL PICKENS

Bachelor of Science in Geology
Oklahoma State University
Stillwater, OK
2018

Submitted to the Faculty of the
Graduate College of the
Oklahoma State University
in partial fulfillment of
the requirements for
the Degree of
MASTER OF SCIENCE
December, 2018

A COMPARISON BETWEEN MODEL AND FIELD

DIESEL MASS RECOVERY IN DOLOMITE KARST

Thesis Approved:

Todd Halihan

Thesis Adviser

Javier Vilcaez

Ahmed Ismail

ACKNOWLEDGEMENTS

I would like to thank my advisor, Dr. Todd Halihan, for providing me the opportunity to work on a unique project and mentoring me throughout the course of this study. I would also like to thank Dr. Javier Vilcaez and Dr. Ahmed Ismail for serving on my committee; Jon Fields and my fellow graduate students at Boone Pickens School of Geology for their assistance and encouragement; and my family and friends for their support and encouragement throughout this project.

In addition, I would like to thank scholarship providers BP American School of Geology and Petroleum division and Chesapeake Energy Geology division. Thanks also need to go out to the members of the City of Ada for their help and providing access to their land and data, with special thanks to Kathy Lippert and Greystone Environmental for providing field data and its interpretation.

I would like to mention a special appreciation for the inspiration Dr. Wayne Pettyjohn provides to me and to others who follow in his footsteps in the field of geology.

Name: CULLEN MIKAEL PICKENS

Date of Degree: DECEMBER, 2018

Title of Study: A COMPARISON BETWEEN MODEL AND FIELD DIESEL MASS RECOVERY IN DOLOMITE KARST

Major Field: GEOLOGY

Abstract:

Analytical subsurface mass removal models are used to evaluate the accuracy and efficiency of remediation approaches. Generally, in field settings, the initial mass of the contaminant source is unknown and thus these analytical approaches cannot be evaluated effectively for complex field conditions. This is more difficult in karst settings, which have preferential flow and perched water tables. At a site near Fittstown, OK, several passive and active remediation technologies were used and monitored after 2000 gal of diesel spilled at an isolated municipal supply well in dolomite. Seven analytical models to estimate hydrocarbon mass attenuation or recovery were tested to predict mass removal of diesel from the various mechanisms that occurred on the site. The analytical predictions of diesel mass removal were either underestimated or overestimated, depending on the remediation technology or attenuation process. Model uncertainties relative to field data mass estimates may be due to parameter sensitivity and variability, sampling methodology, or model assumptions for the analytical solutions. While the models have various uncertainties in mass estimations, they are demonstrated to be useful to provide remediation options and decisions based on these estimates prior to active remediation.

TABLE OF CONTENTS

I: INTRODUCTION 1

II: REVIEW OF LITERATURE 4

Hydrocarbons in Groundwater 4
Fuel in Karst 7
Mass Removal Analytical Models 9
Initial Mass Recovery 9
1) Evaporation: I1 9
2) Excavation: I2 11
Active Mass Recovery 13
3) Submersible Pump-and-Treat: A1 13
4) Skimmer Pump-and-Treat: A2 20
5) Soil Vapor Extraction: A3 23
6&7) In Situ Flushing: A4 & A5 26
Natural Attenuation 28
8) Volatilization: NA1 28
9) Bioremediation: NA2 30

III: SITE DESCRIPTION 33

Geography 33
Climate 33
Geology 35
Hydrogeology 37

IV: SITE CHARACTERIZATION AND REMEDIATION 41

Impact and Initial Response 41
Site Characterization 42
Remediation 47

V: METHODS 49

Field Measurments 49
Initial Mass Recovery 49
1) Evaporation: I1 49
2) Excavation: I2 49
Active Mass Recovery 50
3) Submersible Pump-and-Treat: A1 50
4) Skimmer Pump-and-Treat: A2 51
5) Soil Vapor Extraction: A3 51
6) Surfactant Enhanced Skimmer Pump-and-Treat: A4 52
7) Surfactant Enhanced Soil Vapor Extraction: A5 52
Natural Attenuation Mass Recovery 53
8) Volatilization Estimation: NA1 53
9) Bioremediation: NA2 53
Mass Recovery Modeling 54
Initial Mass Recovery 54
1) Evaporation: I1 54
2) Excavation: I2 55
Active Mass Recovery 56
3) Submersible Pump-and-Treat: A1 56
4) Skimmer Pump-and-Treat: A2 57
5) Soil Vapor Extraction: A3 59
6) Surfactant Enhanced Skimmer Pump-and-Treat: A4 61
7) Surfactant Enhanced Soil Vapor Extraction: A5 62
Subsurface Parameters 62

Natural Attenuation Mass Recovery 64
8) Volatilization: NA1 64
9) Bioremediation: NA2 65
Model Uncertaintiy Evaluations 65

VI: RESULTS 67

Initial Mass Recovery 67
1) Evaporation: I1 67
2) Excavation: I2 68
Active Mass Recovery 68
3) Submersible Pump-and-Treat: A1 68
4) Skimmer Pump-and-Treat: A2 69
5) Soil Vapor Extraction: A3 70
6) Surfactant Enhanced Skimmer Pump-and-Treat: A4 70
7) Surfactant Enhanced Soil Vapor Extraction: A5 71
Natural Attenuation 72
8) Volatilization: NA1 72
9) Bioremediation: NA2 72

VII: DISCUSSION 74

Parameter Variability and Estimation 74
Model Variability 75
Future work 78

CHAPTER VIII: CONCLUSIONS 80

REFERENCES 83

APPENDICES.. 92

LIST OF TABLES

Table 1: Diesel properties used in this study used from literature..... 6
Table 2: Timeline of activities occurred at the site 44
Table 3: Properties for each soil layer used in the API LDRM..... 63

LIST OF FIGURES

Figure Page

Figure 1: Regional scale of the study site 34

Figure 2: Regional geology at the site 36

Figure 3: Potentiometric map of the Arbuckle-Simpson aquifer..... 39

Figure 4: Site map of WW1 40

Figure 5: Development of a conceptual model using electric resistivity and drilling..... 46

Figure 6: Model volume of diesel mass removed.....69

Figure 7: The sum diesel volume removed for each remedial model estimate 73

CHAPTER I

INTRODUCTION

Petroleum fuels are an essential resource in modern society for transportation or electricity. These fuels are transported or stored in tanker trailers, petroleum distilleries, pipelines, and both above ground and underground storage tanks. With the wide variety of transportation and storage, spills and leaks do occur (Etkin, 2009; Ramseur, 2017; U. S. EPA, 2018) and cleanup of these spills is needed to protect human health and the environment (Risher, 1995; Agency for Toxic Substance and Disease Registry, 1996; Udem et al., 2011). Cleanup can utilize natural attenuation through microbial process or active remedial technologies to restore these sites. Predicting which approach would be most effective can be accomplished with several analytical mass removal models developed to predict mass removal of hydrocarbons.

Prior studies have shown the effectiveness of these remedial technologies in the laboratory (Hess et al., 1996; Waddill and Parker, 1997; Chevalier and Petersen, 1999; Schluep, 2000; Lee et al., 2001; Qu et al., 2013; Wang et al., 2014) and in the field (Höhener et al., 1998; U. S. EPA, 2000; Wang and Mulligan, 2004; U. S. EPA, 2005; U. S. EPA, 2005; Rahbeh and Mohtar, 2007; Burden et al., 2008; Chiu et al., 2013; McCoy et al., 2015). Studies for these methods have determined the transport characteristics of the site and specific properties of the contaminant are essential to predict or quantify the mass removal of the contaminant. Several models have been developed for this purpose; some are simple, requiring a basic calculator with few analytical

parameters, while others are complex, requiring advance computing with multiple parameters and a 3-D numerical solution.

Several of these models have not been field tested with a known initial petroleum mass; they use similar field scenarios with estimated initial petroleum mass (Lyman et al., 1981; Johnson et al., 1990; Fingas, 2013; Kuo, 2014; McCoy, 2015).

The purpose of this study is to test uncertainties for mass removal models in a field setting with a known initial mass of contaminant and a known remediated mass for several remedial technologies and methods. A fractured karstic dolomite aquifer impacted by diesel provides a unique field test site to study these uncertainties. A variety of remedial methods were used on the error calibration field site such as excavation, submersible pump-and-treat, skimmer pump-and-treat, soil vapor extraction, *in-situ* soil flushing, evaporation, volatilization, and bioremediation. Each of these have their own advantages and limitations in removing petroleum fuels from a contaminated site. Analytical models have been developed to predict or estimate the mass removed with either estimated or known parameters.

The hypothesis of this thesis is analytical mass removal models for hydrocarbons can be predictive on complex field settings if calibration data for the models are available. By having a test site with a spill of known initial mass into a fractured karstic aquifer and comparing the analytical models predictions with the field recovered mass, the hypothesis can be tested. The background literature will discuss in depth the various technologies and methods used and what models were used for predicting the diesel mass removal. The site description section will discuss the geography, climate, geology, and hydrogeology at the regional and local scale. The site characterization and remediation section will discuss the various methods used to characterize the

site and the remedial work used to extract the hydrocarbon mass at the site with respective dates. The methods section will discuss what instruments and laboratory methods were used in the field and the parameter selection of the models. Results are presented comparing the model and field diesel mass removal, and calculating the error between the model and the field data. Discussion is presented with evaluating uncertainties relating to the parameters, models, or overall conceptual ideas with future work. The final section provides conclusions based on the evaluation of the mass removal models.

CHAPTER II

REVIEW OF LITERATURE

This section reviews literature to provide context for fuel transport, remediation methods, and their analytical models for mass removal. Fuel transport covers how hydrocarbons interact with groundwater and in karst geology. Remediation methods reviews how fuels are removed from the subsurface by using evaporation, excavation, pump-and-treat methods for submersible pumps and skimmer pumps, soil vapor extraction, surfactant flushing, volatilization and bioremediation. Remedial models are discussed with remediation methods to show how the models compute mass removal with each associated remedial method.

HYDROCARBONS IN GROUNDWATER

Hydrocarbon fuel is a complex mixture of saturated aromatic hydrocarbons (Song et al., 2000). Different oil refineries may vary the mix of hydrocarbons in fuels depending on regulations, climate, and season (Dineen, 1991; Song et al., 2000). Diesel is produced as a middle hydrocarbon, with the lighter weight hydrocarbons and most volatile aromatic compounds found in gasoline removed during distillation (Dineen, 1991). The physical and chemical properties of diesel are between lighter hydrocarbons like gasoline and heavier hydrocarbons of crude or bunker oils.

Several physical properties of diesel are needed for transport calculations. The density of diesel is lighter than water but heavier than gasoline, ranging from 0.80-0.86 g/mL (Song et al., 2000), classifying diesel as a light non-aqueous phase liquid (LNAPL). Vapor pressure is the measure of how oil partitions between liquid and gas phases, and is estimated from 1.03-1.38 kPa (Woodrow and Seiber, 1988). The hydrocarbon variability of diesel complicates the measurement of vapor pressure and is rarely used to assess spills (Fingas, 2001). The viscosity of diesel is dependent on the amount of lighter and heavier fractions of compounds (Fingas, 2001), ranging from 2-4 centistokes with most estimates at 2 cm^2/s (Environment Canada, 2017).

Oil/air surface tension is force of attraction or repulsion between oil and air (Fingas, 2001), which can vary based on the temperature. Oil/air surface tension of diesel is 23.8 dynes/cm at 25° C and 26.5 at 15° C (Mercer and Cohen, 1990; Environment Canada, 2017). Oil/water interfacial tension is the force of attraction or repulsion between the molecules of oil and water (Fingas, 2001) and falls between 27-29.4 dyne/cm (Fingas 2001; Environment Canada, 2017). With the addition of viscosity, oil/water surface tension is an indication of the extent and speed of LNAPL spreading (Fingas, 2001). If the LNAPL has a lower interfacial tension, then the lateral extent of LNAPL increases (Fingas, 2001).

LNAPL transport primarily relies on advection or dispersion (National Academies of Sciences, Engineering, and Medicine, 2015). LNAPL transport typically migrates vertically in the subsurface until it reaches an impermeable matrix or the water table. At either of these conditions, the LNAPL will commonly disperse and follow the down gradient pathway of the impermeable layer or the water table interface. Lateral flow by advection is primarily caused by a positive gradient along either an impermeable layer or the direction of groundwater flow (National

	Value	Unit	Source
Density	0.80-0.86	mg/L	Song et al., 2000
Viscosity	2-4	cm^2/s	Environment Canada, 2017
Molecular Weight	234	g/mol	Fogg, 2017
Vapor Pressure	1.03-1.08	kPa	Woodrow and Seiber, 1988
Oil/Air Surface Tension	23.8	dynes/cm @ 25° C	Mercer and Cohen, 1990
	26.5	dynes/cm @ 15° C	Environment Canada, 2017
Oil/Water Interfacial Tension	27-29.4	dynes/cm @ 15° C	Fingas, 2001
			Environment Canada, 2017

Table 1: Diesel properties used in this study used from literature.

Academies of Sciences, Engineering, and Medicine, 2015). Diving plumes with vertical LNAPL movement are also possible (Newell et al., 1995).

Some examples of LNAPL field study sites include Bemidji, MN; Carson and Los Angeles, CA; and Pusan, Korea. The Bemidji, Minnesota site was to observe the subsurface flow, dissolution, volatilization, and bioremediation of approximately 1.7×10^6 L (10,700 barrels) of crude spilled oil evaluated over 30 years of study (Essaid et al., 2011). At the Carson and Los Angeles sites, both surfactants and bioremediation test pilots were conducted for their effectiveness (Los Angeles LNAPL Working Group, 2015). The Pusan, Korea site was to determine the effectiveness of surfactant flushing of diesel at the field scale (Lee et al., 2005).

While hydrocarbon fuels in a porous matrix such as sandstone may disperse in an elliptical shape and flow from pore to pore, fuel transport in karst is different as fuel typically migrates in fractures or conduits (National Academies of Sciences, Engineering, and Medicine, 2015). Advection is the primary transport of both water and fuel in karst. Fractures are the primary pathways for advection unless there is a more permeable flow path (National Academies of National Academies of Sciences, Engineering, and Medicine, 2015). LNAPL accumulates primarily above the water table, but it can be transported horizontally and vertically in fractures beneath the water table (Adamski et al., 2005). This can trap LNAPL beneath or above the water table and allow contamination of remediated groundwater with changing groundwater levels (Newell, 1995). Several factors affect transport such as rock fracture and matrix geometries, local variations in flow velocity, fracture aperture, fracture roughness, and hydrodynamics at fracture intersections (National Academies of National Academies of Sciences, Engineering, and Medicine, 2015).

Remediation of fuel in karst requires a different approach compared to porous media. Difficulties of remediating fuel-impacted karst are primarily in characterization, plume transport, and access to contaminants in the subsurface. Characterization of impacted karst require more detailed characterization and non-invasive techniques (National Academies of Sciences, Engineering, and Medicine, 2015); this may increase the cost and be more difficult for deep impacted areas in competent fractured aquifers. A limited hydrogeological conceptual model might allow the migration of remedial injections away from the impacted portion of a site. Plume extent and flow can cause difficulty in remediation, as fractured pathways are not the same as in porous media.

Transport of the fuel may follow a “stair-stepping” shape where highly transmissive vertical fractures can cause the plume to move to lower or higher areas in the subsurface (National Academies of Sciences, Engineering, and Medicine, 2015).

The depth of the contaminant also varies for possible discharge points. Shallow areas may have discharge points at surface water areas, while a deeper area may hold the contaminants for a longer time scale (National Academies of Sciences, Engineering, and Medicine, 2015). Access to contaminants may pose another difficulty in remediation. If pump-and-treat methods or surfactant injection methods are applied, they might not reach the contaminated area if a flow path with higher transmissivity is available and moves away from the intended area.

Possible technologies used for fuel remediation in fractured aquifers may include pump-and-treat methods, in-situ chemical flushing, or natural attenuation. Pump-and-treat, whether it is a submersible pump, skimmer pump, or vacuum pump, removes the contaminant from the subsurface to an above ground storage unit or disposal area. Pump-and-treat methods rely on advection for transport, the primary transport method in fractured karst systems (National Academies of Sciences, Engineering, and Medicine, 2015). In situ chemical flushing can include water, acidic aqueous solutions, basic solutions complexing or reducing agents, cosolvents or surfactants (U. S. EPA, 2006). The chemical components rely on advection for transport to the contaminated areas (National Academies of Sciences, Engineering, and Medicine, 2015). Natural attenuation includes volatilization, bioremediation, dissolution, and sorption (U.S. EPA, 1999). Volatilization relies on the phase change from liquid to vapor by natural vapor pressure differences. Bioremediation does not rely on the advection process unless injecting microbes or other properties for microbes to grow. Instead, bioremediation relies on the microbes already

present in the subsurface for remediation. Dissolution is the breakdown of complex compounds by water; some compounds degrade more easily than others do.

MASS REMOVAL ANALYTICAL MODELS

Nine types of mass removal analytical models were selected based on the field site remedial history. These are given abbreviations for their use in this work, *I* for the initial phase, *A* for active remediation, and *NA* for natural attenuation mechanisms. Initial passive and active remediation includes evaporation (I1) and excavation (I2). Active remediation includes submersible pump-and-treat (A1), skimmer pump-and-treat (A2 & A4), and soil vapor extraction (SVE) (A3 & A5) before and after the application of surfactants. Before the application of surfactants, submersible pump-and-treat (A1), skimmer pump-and-treat (A2), and SVE (A3) were used. After surfactant flushing, skimmer pump-and-treat (A4) and SVE (A5) were used. Natural attenuation includes volatilization (NA1) and bioremediation (NA2). The following will include detailed descriptions of each method: factors affecting the mass removal calculation, the analytical model selected and which parameters are utilized.

INITIAL MASS RECOVERY

1) EVAPORATION: I1

Evaporation is the first process to occur during and following the diesel spill with the liquid phase changing to a vapor phase (Atkins, 2018). The layer of vapor above the liquid is known as the boundary layer. The boundary layer characteristics may influence evaporation of some liquids, but not petroleum products (Fingas, 2013).

The primary factors for evaporation include temperature and LNAPL thickness. Temperature is the major factor with higher temperatures increasing the rate of evaporation (Fingas, 2013). The thickness of the petroleum affects the evaporation of diesel if the thickness is greater than 2 mm, which increases the path length of volatile components that must diffuse through a thicker layer. If the thickness is greater than 2 mm (3.28×10^{-3} ft), a correction factor can be applied to the calculation of diesel evaporation rate (Fingas, 2013). Wind speed and surface area do not affect the evaporation of LNAPL (Fingas, 2013).

The efficiency and advantages for evaporation is that it occurs naturally and has a high relative evaporation rate compared to unprocessed hydrocarbons. As diesel is a mixture, some compounds of diesel will evaporate quicker than other compounds (Fingas, 2013). Diesel naturally evaporates with the increase of temperature. Most surface spills will evaporate within days if held at constant high temperatures (Fingas, 2013).

There are several disadvantages of mass loss by evaporation; low volatility rate, the presence of heavier organic compounds, parameter changes, and difficulty in field evaluation may be problematic (Fingas, 2013). While diesel may evaporate faster than raw hydrocarbons, diesel has a lower volatility and can evaporate at a slower rate than lighter fuels, such as gasoline, below its boiling point. This is primarily because the heavier hydrocarbons in diesel have lower volatility points than the compounds in gasoline. Field evaluation is also difficult to quantify as various conditions could affect diesel evaporation rates over a large area. This could leave the heavier organic compounds behind after the evaporation of lighter organic compounds. The evaporation of lighter compounds may change diesel parameters such as viscosity, density, and flash point (Fingas, 2013). With the remaining heavier diesel compounds and parameter changes,

remediation prediction and effectiveness may become more difficult (Fingas, 2013). Evaporation is easier to measure in the lab; evaporation measurements in the field are more difficult with varying environmental conditions and large spill sizes.

Fingas created several empirical analytical models based on lab experiments to estimate evaporation rates of gasoline, diesel, and crude oils (Fingas, 2013). While most fuels follow a logarithmic decay curve with time, diesel evaporation rates follow a square root with time decay model (Fingas, 2013). For the diesel evaporation equation, the amount of time diesel has been exposed is required. Two different empirical equations have been used if the diesel has been exposed for more or less than five days. An additional equation may be added if the thickness of the diesel spill is more than 2 mm. The equation used in this study considered diesel exposed for less than five days, with a thickness of less than 2 mm. The equation is:

$$V_{EVAP} = V_t - (V_t \, x \, \%EVAP) = V_t - (V_t x \ (0.39 + 0.13T)\sqrt{t}, \tag{2.1}$$

where V_{EVAP} is the volume of diesel evaporated in L (gal), V_t is the total volume of diesel spilled in L (gal), *%Evap* is the percentage of diesel evaporated, T is the ambient air temperature in °C (°F), and t is the time the diesel was exposed to the ambient air temperature in minutes (Fingas, 2013). The mass of diesel removed can be determined by multiplying the density of diesel with the volume of diesel evaporated.

2) EXCAVATION: I2

Excavation is the removal of contaminated soil from the impacted site to prevent the LNAPL from further affecting the site (Kuo, 2014). Primarily, construction equipment removes soil from a site and disposal trucks remove the impacted soil from the site. Contaminated soil can be placed

directly into the disposal trucks or temporarily stored on an impermeable surface or in a storage unit to prevent runoff of LNAPL. Disposal of contaminated soil is commonly performed by trucking soil to EPA designated disposal facilities. The soil is then either thermally inducted or allowed to let LNAPL evaporate (Kuo, 2014).

Excavation is advantageous due to the relative simplicity of requiring general excavation equipment and no complex understanding of the process (U. S. EPA., 1991). Excavation's generally short time frame can be used as a rapid response option. Additionally, it is useful in low permeability settings (Barnes et al., 2002; U. S. EPA 2012). If the soil has low permeability, excavation can assume that advection of LNAPL doesn't occur on short time scales.

The cost of excavation for equipment, removal, storage, disposal, and labor will increase with time and size of the contaminated area. Excavation is generally limited to the vadose zone as deeper phreatic excavations are costly (Testa and Winegardner, 1990). Excavation becomes problematic for large contaminated areas, significant depth to impacts, and when the total costs are high (Barnes et al., 2002; U. S. EPA 2012). If the size of the contaminated area is too large, excavation time and cost may increase to a point where excavation is ineffective as a remediation option. The depth to bedrock may inhibit excavation, as most excavation equipment is unable to remove the harder bedrock without more expensive equipment or risk the contaminated bedrock spreading impacts (Barnes et al., 2002; U. S. EPA 2012).

Most equations to predict the mass removal of LNAPL by excavation are simple (Kuo, 2014). Parameters usually include volume of pit, average concentration of contaminant, and density of soil and contaminant. Average concentration of the contaminant is taken from multiple soil

samples before the excavation as drill logs, during excavation, or after excavation from a stored pile. The equation for contaminant removal through excavation is:

$$V_{TPH} = \frac{\left(V_{PIT} \times \frac{1}{n} \sum_{i=1}^{n} C_i \times \rho_{SOIL}\right)}{\rho_{LNAPL}}, \quad (2.2)$$

where V_{TPH} is the volume of TPH in m^3 (ft^3), V_{PIT} is the volume of the excavation pit in L (gal), n is the total number of soil samples, i is the sample number, C_i is the concentration of the soil sample i in mg/kg, ρ_{Soil} is the density of the soil in kg/m^3, and ρ_{LNAPL} is the density of the LNAPL in kg/m^3 (Kuo, 2014). The mass of TPH removed by excavation can be determined by multiplying by the density of the LNAPL.

ACTIVE MASS RECOVERY

3) SUBMERSIBLE PUMP-AND-TREAT: A1

Submersible pump-and-treat is a common remediation technique that pumps out contaminants and water from the subsurface to be treated or removed from the site (U.S. EPA, 1996). There are multiple case studies for predicting the effectiveness of pump-and-treat LNAPL contaminant mass removal, field removal, and guidelines (Mackay and Cherry, 1989; McKinney et al., 1996; U.S. EPA, 1996; Cohen et al., 1997; U. S. EPA, 2005; Baú and Mayer, 2008; Burden et al., 2008 Ko and Lee, 2010). Pump-and-treat remediation is a common tool for its simplicity of calculating and field methodology (Mercer, 1990; U.S. EPA, 1996); calculation of contaminant mass removal is similar to water removal and flow rates (Newell et al., 1995). Field methodology is simple with the installation of a well, a pump, and storage containers or treatment system (Mercer, 1990).

Submersible pump-and-treat is considered dual phase pumping of both the aqueous and free phase LNAPL (Mercer,1990). The remediation technique works by creating a cone of depression with the water via pumping (Newell et al., 1995). The floating LNAPL flows with the water in the cone of depression and is pumped out with the water. The cone of depression can be considered as the radius of capture (Newell et al., 1995; Charbeneau, 2007).

Advantages of submersible pump-and-treat remediation includes multiple studies, simplicity, large production rates, and reduction of LNAPL movement (Mercer, 1990; Cohen et al., 1997; Charbeneau, 2007). Submersible pump-and-treat is common and well evaluated in scientific literature, as well as in the regulatory environment (Mercer, 1990). Submersible pump-and-treat requires installing a pump and removing water and contaminant to a disposable container or area (Newell et al., 1995; Cohen et al., 1997). If no well is present, one can be installed at the best possible area to intervene contaminant flow or where the most contaminant is gathered. Submersible pump-and-treat can also achieve large production rates if the permeability is high enough and the pump is capable of high volume pumping rates (Newell et al., 1995; Cohen et al., 1997). If the contaminant is mobile, submersible pump-and-treat can intercept the flow path or make the LNAPL flow toward the well if the hydrogeologic conditions are appropriate (Mercer, 1990; Newell et al., 1995; Cohen et al, 1997).

The disadvantages of submersible pump-and-treat application includes low permeability settings, inability to pump the residual phase of LNAPL, smearing of the recovery well during or post installation, the tailing effect where recovery decreases over time asymptotically, missing the location of the LNAPL in the subsurface, and time limits (Mercer, 1990; Newell et al., 1995; Cohen et al., 1997; Charbeneau, 2007). Submersible pump-and-treat can only remove free-

flowing LNAPL, and is unsuitable for use if the LNAPL is in a low permeable matrix, where contaminant and water flow is restricted. Residual LNAPL is unaffected by submersible pump-and-treat (Mercer, 1990).

Pumping LNAPL out of the well or borehole may cause smearing alongside the well or borehole (Newell et al., 1995). Smearing is caused when drawdown of the water table and floating LNAPL is high enough to cause LNAPL smear along the sides of the well or borehole. When pumping halts, the recently remediated water covers and submerges the smeared region of the well and becomes contaminated again (Newell et al., 1995). Another effect of pump-and-treat is known as tailing. Tailing is a residual factor where free flowing LNAPL is pumped, but leaves a "tail" of residual in the subsurface (Mercer, 1990; U.S. EPA 1996). When the water table recovers, the water is contaminated again with the LNAPL (Mercer, 1990; U.S. EPA 1996).

Another issue in submersible pump-and-treat is the radius of capture missing the flow path of the LNAPL (Mercer, 1990; Cohen et al., 1997). A misplaced recovery well, low pumping rates, or low permeability may cause the radius of capture to miss some or all of the free-flowing LNAPL. In general, continuous pumping has shown decreases in contaminant recovery (Mercer, 1990). Time-step pumping may be used where the water table and LNAPL is allowed time to accumulate around the recovery well for increased contaminant recovery (Mercer, 1990).

The model selected for submersible pump-and-treat is the American Petroleum Institute's (API) LNAPL Distribution and Recovery Model (LDRM) developed by Charbeneau (2007) to determine the saturation, distribution, and potential recovery of LNAPL in the subsurface. The model uses Van Genuchten equations for saturation distribution and Darcian and Theim equations for LNAPL movement and recovery. The model can simulate up to three layers of soil and

recovery simulation for submersible pump-and-treat, dual phase pumping, skimmer pump-and-treat, and trench flow recovery (Charbeneau, 2007).

In order to calculate the model, information on site characteristics, LNAPL properties, soil characteristics, and pumping variables are required (Charbeneau, 2007). Site characteristics data is the depth to water table and any layer intervals; the depths between each interval also determine the thickness of the layers. LNAPL fluid characteristics including density, viscosity, surficial tension between LNAPL and air, and interfacial tension between LNAPL and water are essential data, while viscosity and density of water is all that is required for the water phase. Soil characteristics includes data for each layer require porosity, hydraulic conductivity, van Genuchten parameters "N" and "α", water saturation, and residual saturation f-factor. Once these parameters are known, the saturation distribution of LNAPL is calculated (Charbeneau, 2007). Recovery of LNAPL requires the selection of the recovery method used and associated parameters. The submersible pump-and-treat method requires pumping time, well radius, radius of influence, radius of capture, pumping rate, and saturated thickness to calculate how much diesel is removed (Charbeneau, 2007).

Several equations are used for LDRM. The saturation and distribution of the LNAPL is first calculated at various elevation intervals. Once the model has calculated the elevation values, another set of equations are used for recovery. The following order describes first the saturation and distribution of fluids in the model followed by the recovery.

1) Thickness of LNAPL equation (2.3)
2) The van Genuchten "M" parameter for either Burdine or Mualem models
3) Total liquid effective saturation

4) Total effective water saturation
5) Initial LNAPL saturation for both below and above the air/LNAPL interface
6) LNAPL residual saturation
7) Water saturation
8) LNAPL saturation above and below the air/LNAPL interface
9) Recoverable LNAPL saturation equation (2.4)

The recovery of LNAPL is calculated after selecting the recovery method and inputting the required parameters. The API LDRM is calculated as follows:

1) Relative permeability for either Burdine or Mualem models
2) LNAPL transmissivity equation (2.5)
3) Recovery rate of LNAPL equation (2.7)
4) Parameters "β", "χ", "δ", and "η" for linear
5) Linear equations for recoverable volume and transmissivity equations (2.8) and (2.9)
6) Change of thickness over time equation (2.10)
7) Continuity parameter for submersible pump-and-treat equation (2.11)
8) Thickness of LNAPL at second and third time intervals equation (2.12)

Calculating the distribution and saturation of LNAPL starts with the thickness of LNAPL. The thickness of LNAPL, $b_{n(max)}$, is calculated:

$$z_{max} = z_{an} + \frac{(1-\rho_r)(\sigma_{an}/\sigma_{nw})}{\rho_r-(1-\rho_r)(\sigma_{an}/\sigma_{nw})} b_n, \quad (2.3)$$

where z_{max} is the maximum elevation of LNAPL due to capillary rise (m or ft), z_{an} is the elevation between the air and LNAPL bgs (m or ft), ρ_r is the density ratio between LNAPL and water

(unitless), σ_{an} is the surface tension between air and LNAPL (dynes/cm), σ_{nw} is the interfacial tension between water and LNAPL (dynes/cm), b_n is the thickness of LNAPL (m or ft) (Charbeneau, 2007). Once saturation distribution has been calculated, the amount of recoverable LNAPL is calculated using the saturation of free-phase LNAPL and residual LNAPL. The equation used is:

$$R_n(b_n) = \int_{z_{nw}}^{z_{max}} n(S_n(z) - S_{nr}(z))dz, \tag{2.4}$$

where $R_n(b_n)$ is the recoverable volume (L or gal), z_{nw} is the elevation of the LNAPL and water interface (m or ft), n is the porosity of the layer (unitless), $S_n(z)$ is the saturation of free phase LNAPL at elevation z, and $S_{nr}(z)$ is the saturation of residual LNAPL at elevation z (Charbeneau, 2007).

For the permeability function, there are two different equations based on if the Burdine or Mualem model is used. For LNAPL transmissivity, the equation is:

$$T_n(b_n) = \frac{\rho_r}{\mu_r} \int_{z_{nw}}^{z_{max}} K_{ws}(z)\, k_{rn}(S_w, S_n)dz, \tag{2.5}$$

where $T_n(b_n)$ is the transmissivity of LNAPL at LNAPL thickness (m^2/d or ft^2/d), ρ_r is the density ratio between LNAPL and water (unitless), μ_r is the viscosity of LNAPL (cp), $K_{ws}(z)$ is the hydraulic conductivity of water for selected layer (m/d or ft/d), and $k_{rn}(S_w,S_n)$ is the relative permeability of LNAPL (Charbeneau, 2007) .

The continuity equation for recovering LNAPL can be expressed by:

$$-A_c \frac{dR_n}{dt} = Q_n, \tag{2.6}$$

Where A_c is the area extent of the region of capture for a well (m^2 or ft^2), R_n is the recoverable volume of LNAPL (L or gal), t is time of recovery (days), and Q_n is the recovery rate of LNAPL (L/d or gal/d) (Charbeneau, 2007).

Q_n can further be calculated by:

$$Q_n = \frac{Q_w T_n(b_n)}{T_w(b_w)\rho_r}, \tag{2.7}$$

Where Q_w is the water discharge rate (L/d or gal/d) and $T_n(b_n)$ is the transmissivity of water (m^2/d or ft^2/d) (Charbeneau. 2007). However, there are problems trying to solve equation (2.6). R_n and T_n are nonlinear functions of b_n and cannot be integrated. Instead, piecewise linear equations are used for best fit for both the recoverable volume and transmissivity of LNAP (Charbeneau, 2007).

The linear equation for recoverable LNAPL is:

$$R_n(b_n) = \beta(b_n - \chi), \tag{2.8}$$

with β and χ as constants for recoverable volume and b_n is the thickness of LNAPL (m or ft) (Charbeneau, 2007).

For transmissivity of LNAPL, the equation is:

$$T_n(b_n) = \eta(b_n - \delta), \tag{2.9}$$

with η and δ as constants for transmissivity of LNAPL (Charbeneau, 2007).

To determine the change of thickness over time during pumping, an integral is used by using the constant δ and an additional constant developed for submersible pump-and-treat. The equation used is:

$$\frac{db_n}{dt} = -A_{wj}(b_n - \delta_j), \tag{2.10}$$

with db_n/dt as the change of LNAPL thickness over change of time and A_{wj} as a submersible pump-and-treat constant that includes radius of capture, density, transmissivity and pumping rates (Charbeneau, 2007).

The equation for A_{wj} is:

$$A_{wj} = \frac{Q_w}{\pi R_c^2 \rho_r T_{w-bw}} \left(\frac{\eta}{\beta}\right), \tag{2.11}$$

with Q_w as the water pumping rate (L/d or gal/d), R_c as the radius of capture (m or ft), and $T_{w\text{-}bw}$ as the transmissivity of the thickness of the aquifer (m^2/d or ft^2/d) (Charbeneau, 2007).

For the thickness of LNAPL at the second time interval is calculated with the equation:

$$b_n(t_2) = \delta + (b_n(t_1) - \delta)\exp\left(-A_{wj}(t_2 - t_1)\right), \tag{2.12}$$

with t_1 and t_2 as time interval one and interval two (Charbeneau, 2007).

These equations are repeated for a second time for the third piecewise linear function. Equation (2.4) is the primary equation used to determine the volume recovered with equations (2.7), (2.10), (2.11) and (2.12) used for primarily submersible pump-and-treat method. To determine the mass, the volume recovered can be multiplied by the density of the LNAPL.

4) SKIMMER PUMP AND TREAT: A2

Skimmer pump-and-treat was used for both before and after the application of surfactants. Skimmer pump-and-treat works similar to submersible pump-and-treat but produces little or no water during pumping (Obigbesan et al., 2001). The lack of water production allows easier

treatment as it does not require LNAPL/water separation or water disposal. This also lowers the cost with less treatment (Mayer and Hassanizadeh, 2005). Since there is little or no water production, smearing along the wellbore is minimal with maximum pumping from the skimmer pump.

The disadvantages of the skimmer pump-and-treat are a decrease of effectiveness in low permeability settings, no treatment of residual LNAPL, limited radius of capture, lack of LNAPL flow control, and long remediation times (U.S. EPA, 1996; Mayer and Hassanizadeh, 2005; Interstate Technology Regulatory Council 2009). Skimmer pump-and-treat relies on the advection of LNAPL and if the subsurface has low permeability, the effectiveness of skimmer pump-and-treat method is reduced (U.S.EPA, 1996). Skimmer pump-and-treat can only treat free-phase LNAPL and is unable to treat residual LNAPL.

Most skimmer pumps have low pumping rates, increased remediation times, lower radius of capture, and limited hydraulic control (U.S. EPA, 1996; Mayer and Hassanizadeh, 2005). The skimmer pump may have a small radius of capture and miss the plume by misplaced drilling or miscalculated subsurface properties (U.S. EPA, 1996; Interstate Technology Regulatory Council, 2009). The skimmer pump may not be able to alter the flow path of the LNAPL plume if the pumping rate is too small to adjust for the error. If the extraction well and radius of capture are in the flow path of the plume, the pumping rates of the skimmer pump may not be strong enough to alter all of the LNAPL toward the extraction well and continue down the flow path (U.S. EPA, 1996). Remediation time of skimmer pump-and-treat method may take upward to several months or years as low pumping rates increase the time.

The API LDRM calculator can also predict the recoverable volume of LNAPL using a skimmer pump (Charbeneau, 2007). The inputs for elevations, layer thickness, fluid characteristics, and soil characteristics are the same as those used for submersible pumping. The only change is the selection of skimmer pump-and-treat and the inputs required for the recovery calculation (Charbeneau, 2007). The inputs for skimmer pump-and-treat is the type of aquifer being remediated, remediation time, the radius of capture and the well of the skimmer pump. The equations calculating saturation, permeability, transmissivity, and recoverable volume are the same (Charbeneau, 2007). Only equations (2.7), (2.10), (2.11) and (2.12) are changed for the application of skimmer pump-and-treat (Charbeneau, 2007). The recovery rate for skimmer pump-and-treat is:

$$Q_n = \frac{2\pi(1-\rho_r)T_n(b_n-b_{nw})}{\ln(R_c/R_w)}, \tag{2.13}$$

Where b_{nw} is the LNAPL thickness in the well constrained by a fine grain zone (FGZ) (m or ft) and R_w is the radius of the extraction well (m or ft) (Charbeneau, 2014).

The continuity equation for the skimmer pump-and-treat method is:

$$\frac{\mathrm{db_n}}{\mathrm{dt}} = -\mathrm{A_{sj}}(\mathrm{b_n} - \delta)(\mathrm{b_n} - \mathrm{b_{nW}}), \tag{2.14}$$

with A_{sj} as the skimmer pump-and-treat performance coefficient and b_{nw} thickness of the water table (m or ft) (Charbeneau, 2007).

The performance coefficient equation is:

$$A_{sj} = \frac{(1-\rho_r)}{R_c^2 ln\ (R_c/R_w)} \left(\frac{\eta}{\beta}\right), \quad (2.15)$$

(Charbeneau, 2007). The performance equation used is:

$$\mathrm{A_{sj}(t_2 - t_1)} = \frac{1}{\delta - \mathrm{b_{nW}}} \ln\left(\frac{((\mathrm{b_n(t_1)} - \delta)(\mathrm{b_n(t_2)} - \mathrm{b_{nW}}))}{((\mathrm{b_n(t_2)} - \delta)(\mathrm{b_n(t_1)} - \mathrm{b_{nW}}))}\right), \quad (2.17)$$

Where t_1 and t_2 is time interval and $b_n(t_1)$ and $b_n(t_2)$ is the LNAPL thickness at time interval 1 and 2. Equation (2.17) is used to calculate the removal of LNAPL in the subsurface over the given time of remediation (Charbeneau, 2007). Equation (2.4) is used to determine the volume recovered with equations (2.13) to (2.18) used for the constants specifically used for skimmer pump-and-treat method. The mass of LNAPL recovered can be determined by multiplying the volume recovered with the density of the LNAPL.

5) SOIL VAPOR EXTRACTION: A3

Soil vapor extraction or SVE is a similar to the pump-and-treat method for the vapor phase (Mercer et al., 1990). SVE uses vacuums to extract volatile contaminants from the subsurface into either a container or the atmosphere if it the contaminant vapor is safe or treated (Johnson et al., 1990; Anderson, 1994; Newell et al., 1995). SVE also induces volatilization by lowering vapor pressure in the subsurface and encourages more contaminants to transfer from either residual or free phase to the vapor phase (Johnson et al., 1990; Anderson, 1994). With the removal of vapor contaminants, any aerobic microbial colonies that are present in the subsurface can utilize the additional available oxygen (also known as bioventing) (Anderson, 1994).

Advantages for SVE include the remediation of residual LNAPL, volatilization enhancement and bioremediation enhancement (Johnson et al., 1990; Mercer et al., 1990; Anderson, 1994; Newell

et al., 1995). SVE is able to remediate residual LNAPL as it induces the LNAPL from the sorbed phase to gas phase for remediation (Mercer et al., 1990). If the vacuum pressure is high enough, it may be able to also vacuum up free-phase LNAPL but at a lower rate than a submersible or skimmer pump. SVE lowers the partial pressure of the fuel in the subsurface during and after the application (Anderson, 1994; Newell et al., 1995). SVE is able to induce volatilization during and after the method has been applied (Anderson, 1994; Newell et al., 1995); some complex compounds may require SVE to volatilize, as they cannot naturally. Bioremediation may also be induced after the application of SVE (Anderson, 1994; Newell et al., 1995). With the removal of contaminants and flow of oxygen in the subsurface, aerobic microbes are allowed to grow and remove the remaining contaminants (Newell et al., 1995). This will continue remediation of primarily the residual phase LNAPL (Newell et al., 1995).

Soil vapor extraction has similar disadvantages to other pump-and-treat methods with low permeability and water table fluctuations. However, SVE is different from other pump-and-treat systems with contaminant concentration changes and the overall vapor pressure threshold increasing during SVE, which can decrease the efficiency of SVE (Johnson et al., 1990; Mercer et al., 1990; Anderson, 1994; Newell et al., 1995). Like most treatment methods that rely on advection, low permeability can reduce the movement of airflow during extraction (Newell et al., 1995). If the SVE pumping is too high, it might cause water table fluctuations in the subsurface and smear against the well sides when pumping ceases (Johnson et al., 1990). Unlike most pump-and-treat methods that can remove the entire LNAPL, SVE relies on the vapor pressure of the contaminant. If the contaminant cannot naturally volatilize or have low enough vapor pressures to be induced by SVE, then the method cannot remove the contaminant (Newell et al., 1995). If the

contaminant is a complex mixture with multiple compounds, each with different vapor pressures, SVE may induce the volatilization of only the compounds with low enough vapor pressures and leave the remaining compounds (Johnson et al., 1990). This could overall change the composition of the contaminant, altering the properties of the contaminant itself and making contaminant removal predictions more difficult (Johnson et al., 1990).

To help predict if SVE is applicable and determine the amount of vapor mass removal, Johnson et al. (1990) created several equations. These equations help estimate the vapor concentration in the subsurface, the required pumping rates, and how much vapor can be removed. First step is to estimate the vapor concentration in the subsurface. This could be done by taking vapor readings at a well, or by estimation using the following equation:

$$C_{est} = \sum_i \frac{x_i P_i^v M_{w,i}}{RT}, \tag{2.19}$$

where C_{est} is the estimated contaminant vapor concentration in mg/L, x_i is the mole fraction of component i in liquid phase residual, P_i^v is the pure component vapor pressure at temperature T in Pa; $M_{w,i}$ is the molecular weight of component I in mg/mole, R is the gas constant in L·Pa/mol·°K, and T is the absolute temperature of residual in °K (Johnson et al., 1990). If multiple components are in a mixture, the mole fraction, vapor pressure, and molecular weight for each component found then summed for an estimated mixture. If only one component is available, x_i will equal 1.

Next is to determine realistic pumping rates using the following equation:

$$Q = H\pi \frac{k}{\mu} p_w \frac{\left[1-(P_{Atm}/P_w)^2\right]}{\ln(R_w/R_I)}, \tag{2.20}$$

where Q is the pumping rate in cm^3/s (ft^3/s), H is the thickness of the well screen in cm (ft), k is the soil permeability to air flow in cm^2 (ft^2), μ is the viscosity of air in g/cm-s, p_w and P_w are the absolute pressure at the extraction well in $g/cm\text{-}s^2$ or atm (psi); P_{atm} is the absolute ambient pressure in $g/cm\text{-}s^2$ or atm (psi), R_w is the radius of vapor extraction well in cm (ft), and R_I is the radius of influence in cm (ft) (Johnson et al., 1990).

Once these two estimations are known, estimated removal rates can be calculated using the equation:

$$R_{est} = C_{est} Q, \tag{2.21}$$

with R_{est} of the estimated removal rate of the estimated vapor concentration (C_{est}) at a certain pumping rate (Q) in units of mass/time (mg/s or lbs/s) (Johnson et al, 1990). The removal rate can be multiplied by the time of pumping to determine the mass. The volume of vapor removed can be divided by the density of the LNAPL in the vapor phase.

6&7) IN SITU FLUSHING: A4 & A5

In situ flushing is a process that involves injection of an aqueous solution through vertical wells or trenches, into contaminated zone. In situ flushing uses surface-active-agents or surfactants. Surfactants are chemical compounds frequently used in detergents and food products that alter the properties of solution interfaces (Sabatini et al., 1995; Strbak, 2000). Surfactants primarily lowers the interfacial tension between non-aqueous phase liquids and water by consisting of a molecular hydrophilic “head” and hydrophobic “tail” that separates the NAPL and water (Cole, 1994). At some instances, tracers have been known to reduce interfacial tension such as the Martel et al. (1996) study where interfacial tension for diesel reduced from 24.6 μN/m to 19.6 μN/m.

Surfactants can lower the interfacial tension of diesel to less than 10^{-3} μN/m (Pope and Wade, 1995; Martel et al., 1996).

The advantage to surfactant flushing is the ability to enhance and mobilize residual LNAPL and encourage bioremediation (Anderson, 1993). With the application of surfactants, most pump-and-treat methods are improved by enhancing the mobilization of free-phase LNAPL. Residual LNAPL is separated from soil particles and flushed with surfactant or water. Some surfactants are also compatible with bioremediation. Microbes can nourish off the surfactant and possibly, off any remaining LNAPL; this eliminates the need to remove the surfactant.

Disadvantages of surfactant flushing are limited effectiveness in low permeable settings, permeability reduction, groundwater chemical reactions, biodegradability, negative impact on bioremediation, and failing to separate LNAPL and water (Anderson, 1993). If the permeability is low, the surfactant will have difficulty flowing through the subsurface at a reasonable rate. Some surfactants may also lower the permeability of the subsurface based on the surfactant composition (Anderson, 1993). The chemical composition of the surfactant may react with the groundwater chemistry and cause additional problems. If the surfactant is biodegradable, it may degrade at a rate faster than it could flush the NAPL out of the subsurface (Speight and Arjoon, 2012). If the surfactant is not biodegradable, it may reduce bioremediation by cleaning out the microbes during, and possibly after flushing (Brusseau et al., 1995; Rouse et al., 1995). The inability to separate the NAPL and water from each other for enhanced NAPL mobility may limit the effectiveness of the surfactant (Anderson, 1993). In some instances, the surfactant is unable to separate the LNAPL from the water or soil grains, rendering the surfactant useless.

Due to the variability and complexity of surfactant flushing, simple analytical equations have not been fully developed for surfactant flushing. Instead, efficiency equations to measure estimated initial contaminant mass and recovered mass after surfactant flushing are used (Pope and Wade, 1995). If the amount of contaminant mass and surfactant mass are known before remediation and after recovery, the efficiency can be used to determine if surfactant should still be applicable to the site (Khalladi et al., 2009). However, they cannot accurately predict contaminant mass removed from the subsurface. It is assumed that surfactant reached the contaminated areas and successfully mobilized the residual LNAPL. The diesel at the site is recovered by using skimmer pump-and-treat and soil vapor extraction. The interfacial tension between LNAPL and water can be reduced to simulate surfactant flushing to predict diesel removal using the LDRM model for skimmer pump-and-treat. Using Johnson's (1990) method, permeability can be reduced to simulate the permeability reduction occasionally shown in surfactant application.

NATURAL ATTENUATION

8) VOLATILIZATION: NA1

Volatilization is the process of converting a chemical from a liquid or solid phase to the vapor phase directly proportional to relative chemical vapor pressures (Kang, 1993; Gordon and Murray, 2014). Volatilization is dependent on the vapor pressure of the chemical and environmental conditions affecting evaporation such as soil moisture (Calabrese and Kostecki, 1991). Adsorption of a chemical onto soil particles reduces the vapor pressure of the chemical due to decrease of chemical activity. Soil moisture may have the opposite affect by transporting

the chemical to the air or water surface where the chemical can volatilize more readily (Calabrese and Kostecki, 1991).

Volatilization has the advantages of being a natural process and can be induced and/or enhanced by SVE (Cole, 1994; Zheng et al., 2004). If the NAPL has a low enough vapor pressure, it can naturally volatilize without human interaction. Most common LNAPL's that can easily volatilize are gasoline, jet fuel, and aviation gasoline (Cole, 1994). If the vapor pressure for the LNAPL is not low enough to volatilize naturally, it can be induced by increasing temperature or decreasing pressure by removing vapor like SVE (Gordon and Murray, 2014). The LNAPL can continue to volatilize shortly after an SVE event until the subsurface vapor pressure reaches its previous vapor pressure. If the LNAPL is volatilizing, SVE can enhance the volatilization of LNAPL and decrease clean–up time.

Disadvantages for diesel volatilization include having low volatility rates, trapped by low permeability layers, and overall low mass reduction for diesel (Cole, 1994). Diesel has low volatility rates that make volatilization and SVE less effective. Contaminant vapors can volatilize and leave the subsurface either by diffusion or advection (Kang, 1993). Low permeability layers may trap the contaminant vapors in the subsurface and make remediation more difficult; while diesel's lighter compounds volatilize faster, diesel's heavier compounds remain.

Hamaker (Lyman et al, 1981), Fingas (2013), and Ma et al. (2014) measured volatilization rates as a function of the inverse of the square root of time. To predict the estimated mass removal of contaminants via volatilization, Hamaker (Lyman et al., 1981) created two simple equations. One equation can predict volatilization through dry soil without water flow intercepting the path,

while the other equation predicts volatilization through soil as water flows through the airflow path. The equation to predict volatilization through dry soil without water flow is:

$$M = A\ x\ Q_t = A\ x\ 2c_0\sqrt{Dt/\pi}, \tag{2.22}$$

with M is the mass removed by volatilization in kg (lbs.), A is the area of the spill beneath the soil in m^2 (ft^2), Q_t as the total loss of chemical per unit area over time in kg/m^2 (lb/ft^2, c_0 the initial concentration in the soil in g/L (lb/gal), D as the diffusion coefficient of vapor through the soil in m^2/s (ft^2/s), and t is the time chosen for vapor to diffuse in seconds (Lyman et al., 1981). Thickness of the subsurface is assumed to be semi-infinite. If volume is needed, the mass of diesel can be divided by the density of diesel.

9) BIOREMEDIATION: NA2

Bioremediation is the remedial method of using living organisms to reduce or eliminate environmental hazards (Speight and Arjoon, 2012). Bioremediation primarily works by using metabolic or enzymatic processes to transform the contaminants to less harmful products or as carbon dioxide, water, and cell biomass. Some material can be degraded anaerobically, with most degraded aerobically (Speight and Arjoon, 2012).

Bioremediation can occur naturally but can be enhanced by biosimulation and bioaugmentation (Speight and Arjoon, 2012). Biosimulation adds nutrients and other substances to catalyze the indigenous microbes. Bioaugmentation implements non-native microorganisms (sometimes genetically altered) to the contaminated site for remediation.

Surfactants that have been applied at a contaminated site may enhance or reduce bioremediation. Some surfactants are called biosurfactants, which lower interfacial tension but are biodegradable and non-toxic to microbes (Speight and Arjoon, 2012). The surfactants may inhibit growth of microbes by either removing the food source (contaminants) or the microbes themselves (Brusseau et al., 1995; Rouse et al., 1995).

Bioremediation is naturally occurring, environmentally friendly, and generally a low cost solution (Speight and Arjoon, 2012). Microbes are already present in the ground and, with the addition of contaminants, can begin to grow and remove the contaminants. Bioremediation is considered environmentally friendly, as the site remediation doesn't disrupt the natural habitat at the surface by the introduction of chemicals or remediation process. Contaminated soil and diesel do not need to be transported off the site, reducing the cost and energy of remediation (Speight and Arjoon, 2012).

Bioremediation is a slow remedial process that might not be suitable for quick remediation (Speight and Arjoon, 2012). Other disadvantages include low permeability trapping carbon dioxide or methane gasses, environmental dependences, and the requirement for degradable compounds (Speight and Arjoon, 2012). If permeability is too low, the CO_2 that microbes emit will be trapped in the subsurface and "choke" the microbes (Anderson, 1994). Environmental dependences include temperatures, pH, and nutrients (Speight and Arjoon, 2012); the optimal temperature for biodegradation is from 25-45° C (77-113° F) (Nester et al., 2001). Nutrients such as phosphorus and nitrogen are needed to allow microorganisms to grow. If there are too many nutrients, the microbes may choose to react to the already present nutrients instead of the contaminant. Another problem relies with the contaminant's biodegradability, while microbes

might thrive in the subsurface without the presence of contaminates, the contaminant may not be degraded if it is too difficult to receive nutrients from the bioremediation process.

Bioremediation can be measured using a method developed by McCoy (2015). McCoy designed CO_2 traps to adsorb the CO_2 for measurement. The CO_2 traps use carbon disks to adsorb escaping CO_2 from the contaminant plume or uncontaminated soil. The traps are processed in the lab to determine the concentration over the area of the disk for the length of time deployed. They are then converted to volume over area over time by using stoichiometric conversion flux. To determine the volume of diesel removed by remediation, the estimated LNAPL loss of volume over area over time can be multiplied by the impacted area and time of traps deployed. The volume of diesel loss by bioremediation can be multiplied by the density of the LNAPL to calculate the mass of diesel loss by bioremediation.

CHAPTER III

SITE DESCRIPTION

The site for this study is a dolomite karst aquifer impacted by a known quantity of diesel over a short time period. This section reviews the geography, climate, and geology of the site to provide a context. The hydrogeology of the aquifer and the wells for the study site are also detailed.

GEOGRAPHY

The site is located in south-central Oklahoma in Pontotoc County (Figure 1). The nearest town to the site is Fittstown, located 6.5 km (4.0 miles) northeast of the site. The site is located at the southern section of the Ada Water Well field at 34.564° N, 96.670° W. The well of the initial diesel impact is named Water Well 1 (WW1).

CLIMATE

The nearby Fittstown Mesonet weather station monitors and records real-time weather events (Figure 1). The station is run by the Oklahoma Climatological Survey, University of Oklahoma, and Oklahoma State University. It is designed to measure the environment and duration of mesoscale weather events (Brock et al, 1995; McPherson et al., 2007). The Fittstown Mesonet Station is located approximately 4.5 km (2.8 miles) southwest of WW1.

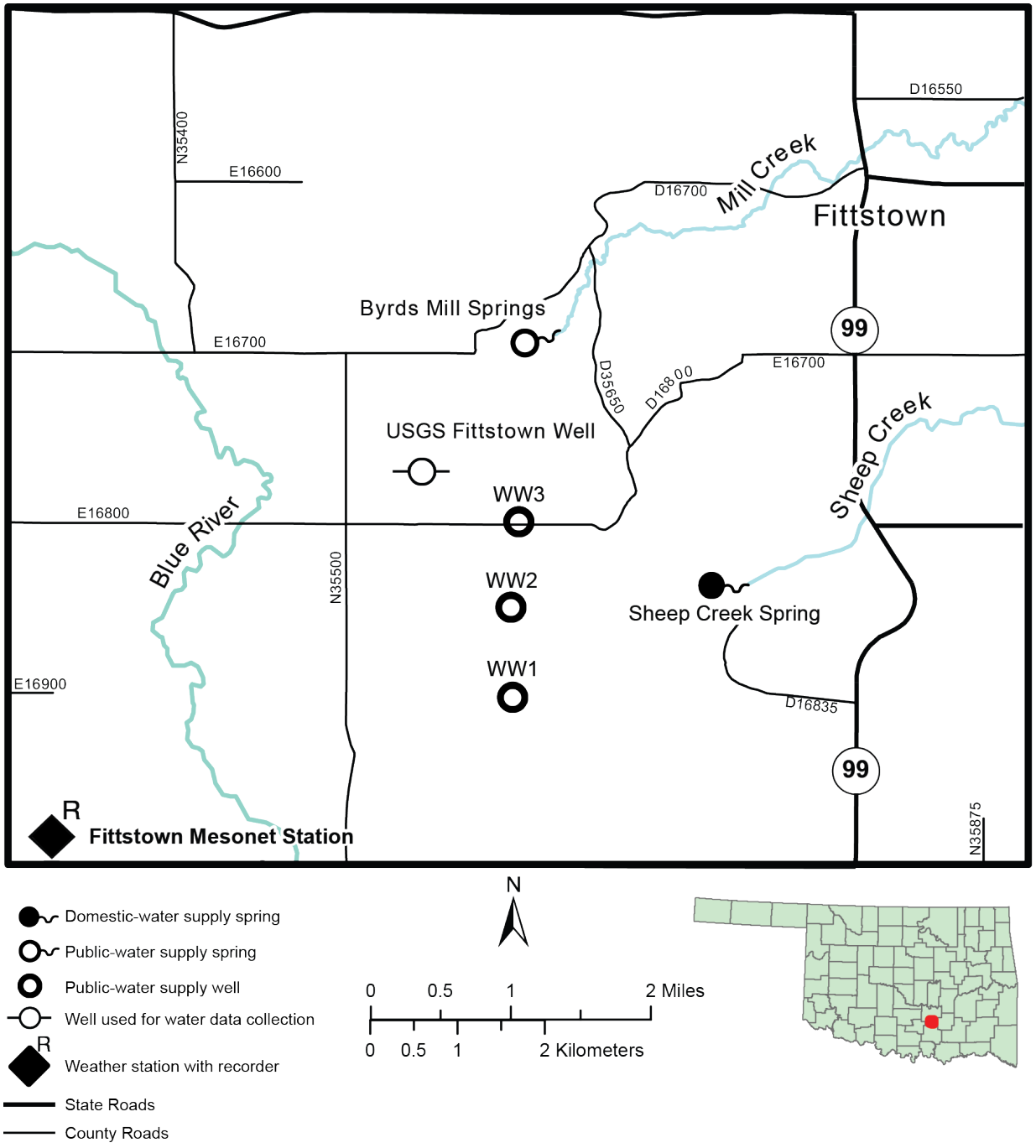

Figure 1: Regional scale of the study site.

Average precipitation on a 30-year average from 1907-2000, ranges from 1070 mm (3.5 ft) to 1140 mm (3.7 ft) per year with the highest rainfall occurring during May and June. Most winters have a minimum of 25 mm (0.08 ft) of snowfall (Oklahoma Climatological Survey, 2010). During the possible span of the spill, total precipitation was 219 m (0.71 ft) and during times of remediation the total amount of precipitation was 2159 mm (7.1 ft) (Brock et al, 1995; McPherson et al., 2007). Over the two year span, from the filling of the above ground storage tanks to the date of non-detect, precipitation was 3512 mm (12 ft). The average temperature is 17° C (62.6° F) with slight variation from south to north in the county. Average high temperature is 34° C (93.2° F) in July and August and an average low of -2.2° C (28.0° F) in January (Oklahoma Climatological Survey, 2010). South to southeast winds are dominant, averaging around 4 m/s (13.1 ft/s) (Oklahoma Climatological Survey, 2010). During the unknown spill time, lowest temperature was -10° C or 14° and the highest temperature was 29° C or 84.2° F. The average temperature during possible spill time was 9° C or 48.2° F (Brock et al, 1995; McPherson et al., 2007).

GEOLOGY

The geology of the site consists primarily of the Arbuckle group (Fig 3); a fractured dolomite karst (Christenson et al., 2011), which has a thickness of approximately 900 m (2953 ft), near the study area. Although the Arbuckle group extends across the state, it is not exposed over much of

it. Most of the Arbuckle group across the state is drilled more for hydrocarbon activities and is highly saline, while the Arbuckle group at the study site is a thick, freshwater aquifer

The surface at the site is weathered Arbuckle group epikarst with very little soil and an average thickness of approximately 8 m (26.2 ft) (Christenson et al., 2011; Greystone Environmental et al., 2016a). Soil at the site is primarily of Scullin gravelly loam and sandy clay with a thickness of less than approximately 1 m (3.3 ft) ((Bogard, 1973; Greystone Environmental et al., 2016a). The formation at the site is lightly fractured. There are no significant mapped faults intersecting at the site (Christenson et al., 2011). The Arbuckle group is primarily a fracture aquifer with several karst characteristics such as small caves near the surface. Video recording shows that the wells in the Ada well field produce from large, deep voids at depths greater than

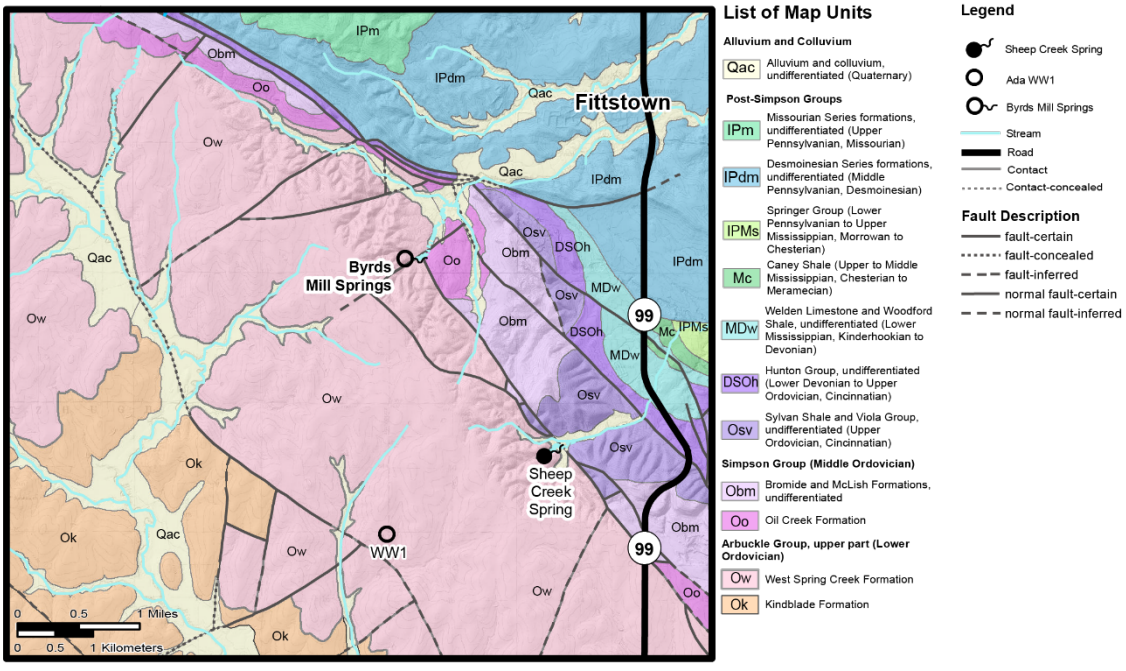

Figure 2: Regional geology at the site (Lidke and Blome, 2017).

200 meters (656 ft). Folding and faulting in the aquifer are significant, but not in the regional of the Ada well field (Christenson et al., 2011).

HYDROGEOLOGY

The Arbuckle-Simpson aquifer is a 1,400 km^2 (1.5 x 10^{10} ft^2) area semi-confined aquifer that spans across Carter, Coal, and Johnston, Murray, and Pontotoc counties (Christenson et al., 2011). The hydrogeology of the site has several studies on the local aquifer (Ham, 1973; Fairchild et al., 1990; Christenson et al., 2011). The Arbuckle-Simpson aquifer is mapped into the eastern, central, and western sections (Christenson et al., 2011). The site is in the eastern Arbuckle-Simpson aquifer, the largest and most studied section of the three. The area is uplifted by the Hunton Anticline, formed during faulting and uplift during the Pennsylvanian.

The site aquifer properties are characterized on the regional and well scales. The regional transmissivity of the Arbuckle-Simpson studies of both Fairchild (1990) and Christenson (2011) is estimated to be 1,110 m^2/d (11948 ft^2/d). A separate aquifer test was conducted to determine any connectivity and contaminant movement of Water Well 1 to Water Well 2 and Water Well 3. Transmissivity determined from this aquifer test is 1,210 m^2/d (13024 ft^2/d) (Pickens and Halihan, 2016).

Storativity of the Arbuckle-Simpson aquifer is variable in previous studies. Fairchild (1990) and Christenson (2011) determined the aquifer storativity to be 0.005 and 0.011, respectively. The aquifer test conducted in 2016 determined the storativity in the Ada wellfield to be 0.014 (Pickens and Halihan, 2016). The gradient direction, for both the well and regional scales, is toward the southeast as shown in Figure 3 (Christenson et al., 2011; Greystone Environmental et al., 2016a).

Several nearby springs provide discharge from the Arbuckle-Simpson aquifer (Christenson et al., 2011). Sheep Creek Spring is a spring on private property approximately 2.4 km (1.5 miles) east of the Ada Well Field. Byrds Mill Spring is a municipal water supply spring for the city of Ada, OK located 3.5 km (2.2 miles) northeast of the well field. Both springs have recording stations monitored by the United States Geological Society (USGS) at the Oklahoma Water Science Center (U.S. Geological Survey, 2016).

There are several wells near the impacted well and at the study site. Three municipal supply wells provide water to the City of Ada during drought conditions. One USGS monitoring well exists to the northwest of the site. Water Well 1 (WW1), Water Well 2 (WW2), and Water Well 3 (WW3) are spaced approximately 0.8 km (.5 miles) from each other in a south-to-north trend (Fig 4). The depths of WW1, WW2, and WW3 are 316 m (1037 ft), 293 m (961 ft), and 280 m (919 ft), respectively. The USGS monitoring well 01N-06E-04 CAD (the Fittstown monitoring well) is located approximately 2.3 km (1.4 miles) northwest of the Ada Water Well Field. The Fittstown monitoring well provides recorded water table data on a five-minute interval.

At the WW1 site, the perched water table is at 10-12 m (33-39 ft) below ground surface (bgs) and the regional water table is at 30 m (98 ft) bgs. There are three deep site monitoring wells CD-03, CD-05, CD-06 to the regional water table. Each of the three wells drilling locations were determined by electric resistivity imaging (ERI) along possible faults and fractures as possible flow paths (Greystone Environmental et al., 2016a). CD-03, CD-05, and CD-06 were drilled to a depth ranging from 43 m (141 ft) to 46 m (151 ft).

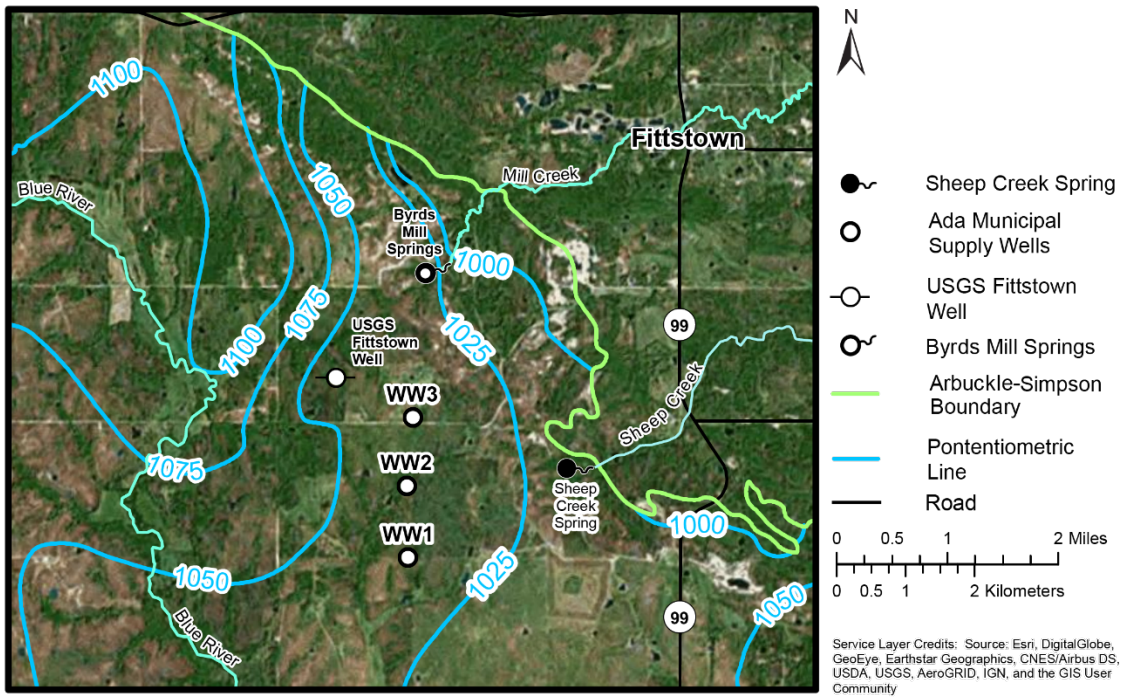

Figure 3: Potentiometric map of the Arbuckle-Simpson aquifer. Flow is toward east-southeast direction.

Around WW1, several shallow remediation wells and trenches were installed for SVE and surfactant flushing through the epikarst or to the perched water table. Six wells were drilled for SVE remediation. The wells were drilled to a depth ranging from 6 m (20 ft) to 12 m (39 ft). For surfactant flushing, five wells (two injection wells and three extraction wells) and three trenches were installed. The two injection wells were drilled to a depth of 1.5 m (4.9 ft), the three extraction wells were drilled to approximately 12 m (39.4 ft), and the three trenches were dug to approximately 1 m (3.3 ft).

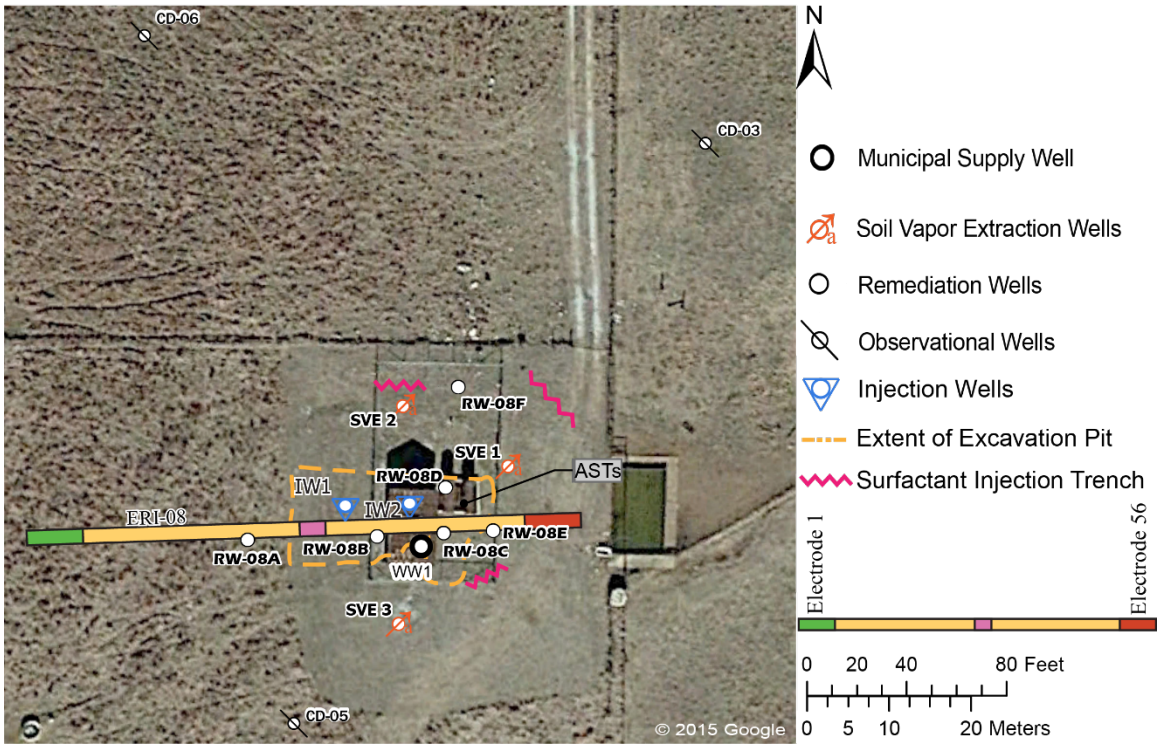

Figure 4: Site map of WW1 with observation wells, remediation wells, and injection wells (Greystone Environmental et al., 2016a; Greystone Environmental et al., 2016b).

CHAPTER IV

SITE CHARACTERIZATION AND REMEDIATION

Two, 1000-gallon aboveground diesel tanks spilled outside of their secondary containment, onto the land surface in an isolated area with little soil and no trees. The only structures in the area were the tanks and a well house with a 366 m (1200 ft) deep municipal supply well (WW1). The diesel impacted the well during the late winter of 2015 with several remedial methods applied from mid-2015 to late 2016. The remediation of the site included an initial emergency response, site characterization, followed by remediation. Diesel samples collected at the site were nondetect for diesel impacts as of June 26, 2017. This section details the initial response, the integrated site characterization, and the remediation of the diesel impact.

IMPACT AND INITIAL RESPONSE

On January 16, 2015, two connected 1,000 gallon above ground storage tanks were filled with diesel (Greystone Environmental et al., 2016a). On April 19, 2015, the tanks were discovered to be empty during a maintenance check. On April 21, 2015, remediation began with excavation of the contaminated surface area around the tanks. The soil was removed and the dolomite epikarst of the site was excavated to an average depth of 2.4 m (8 ft) (depth of competent bedrock) over an area of approximately 10.7 m (35 ft) by 15.8 m (52 ft). The 137.6 m^3 (180 cubic yards) of impacted material were sent to a hazardous waste landfill. The sides of the excavation pit and the excavated material were tested for total petroleum hydrocarbons (TPH). On May 7, 2015, 0.76 m of diesel was measured in WW1 with an interface probe (Greystone Environmental et al., 2016a).

Initial sampling of WW1 indicated 5.1 mg/L of diesel by using EPA method 1664A (Greystone Environmental et al., 2016a).

On May 28, 2015, submersible pump-and-treat remediation began in the water supply well (WW1) and continued until September 15, 2015.

SITE CHARACTERIZATION

Site characterization was conducted by utilizing specialized electrical resistivity imaging (ERI) surveys, confirmation borings, and well sampling. These data were integrated to develop the conceptual site model. The objective of the characterization was to determine the extent of the impacts and the preferential pathways to the impacted wells and away from the site. The ERI was able to determine the horizontal and vertical extent of the diesel light non-aqueous phase liquid (LNAPL) as a resistive portion of the datasets beneath the tank area. The pathways and weathered epikarst were determined to be conductive portions of the ERI datasets. The electrical data indicated the diesel flowed vertically through the epikarst until the diesel reached the perched water table at a depth of approximately 10 meters (30 feet) (Greystone Environmental et al., 2016a). The diesel remained there until it began to flow through a fracture into WW1 to the regional water table at 30 meters (100 feet). The separate phase diesel remained near WW1 and did not migrate more than 7.6 m (25.0 ft) away from the well (Greystone Environmental et al., 2016a).

Drilling logs obtained during well installation confirmed the ERI results. A photoionization detector calibrated to iso-propane measured vapor concentrations from the wells. Fluid sampling, during and after well installation, confirmed a perched water table at a depth of approximately 10-

12 m (33-39 ft) bgs. The chemical data collected from the perched aquifer was used to determine the degree of contamination of that zone. The regional water table for the eastern Arbuckle-Simpson aquifer was sampled at WW1 and three additional monitoring wells placed in the fracture network around WW1 evaluating the water table at a depth of approximately 30 m (98 ft) bgs. Lithological logs collected at several depth intervals during drilling, confirmed the depth and concentration of diesel at each interval.

Based on the ERI and boring data, a conceptual model was determined for the vertical and lateral extent of the diesel (Greystone Environmental et al., 2016a). The diesel impact can be described by vertical and lateral extent of the free phase diesel and residual phase diesel. The vertical extent of the diesel remained primarily under the concrete platform of the above ground diesel storage tanks (Greystone Environmental et al., 2016a). Free phase diesel flowed straight down toward the perched water table. Residual diesel, trapped in soil pores and epikarst fractures, outlines the footprint of the vertical flow path through the shallow portion. In the deeper aquifer, vertical extent of the free phase diesel is controlled by the fracture, which allowed the diesel to flow past the 6.10 m (20 ft) well casing and into the open borehole. Liquid diesel flowed into the open borehole to the deeper water table. The flow path of free phase diesel is shown by the remaining residual diesel trapped by sorption and fractures.

Date	Activity
4/21/2015	Excavation
5/28/2015	Submersible Pump Installed
7/15/2015	Electric Resistivity Imaging Characterization
7/1/2015	Submersible Pump Removed Skimmer Pump Installed
9/17/2015	Drill Wells CD-03, CD-05, CD-06, CD-8a, CD-8b, CD-8c
12/7/2015	Drill Wells CD-8d, CD-8e, CD-8f
12/14-17/2015	Soil Vapor Extraction
1/13-16/2016	Soil Vapor Extraction
1/27-29/2016	Soil Vapor Extraction
3/28/2016	Drill Wells RW1-3 and I1 and I2
4/1/2016	Dig Pits, Surfactant Flush
4/5/2016	Soil Vapor Extraction with 3% Surfactant Solution and Freshwater Flush
4/8/2016	Soil Vapor Extraction with 3% Surfactant Solution and Freshwater Flush
5/10-11/2016	Soil Vapor Extraction with Freshwater Flush
6/1/2016	Soil Vapor Extraction
7/28/2016	Soil Vapor Extraction
8/31/2016	Soil Vapor Extraction
10/6/2016	Soil Vapor Extraction
11/8/2016	WW1 Recased to 46 m

Table 2: Timeline of activities occurred at the site (Greystone Environmental et al., 2016a; Greystone Environmental, 2016)

The lateral extent of the diesel was limited by the preferential downward flow toward the regional water table (Greystone Environmental et al., 2016a). Free phase diesel flowed toward WW1 and stayed around the well, with the well acting as a sump (Greystone Environmental et al., 2016a). After the diesel flowed past the well casing and dropped into the open borehole, the free phase diesel remained around WW1 and could only extend laterally by connected fractures, which followed the groundwater flow away from the site (Greystone Environmental et al., 2016a). The residual phase diesel only moved laterally from the well when the water table dropped significantly, generally at the end of summer.

Post remediation characterization was evaluated with a temporal ERI dataset and well vapor readings. Bioremediation was determined to occur with ERI using a differencing image conducted on June 17, 2015, before remediation (Figure 5) and December 16, 2016, after remediation (Figure 5). The temporal ERI dataset showed a change of nearly 300% from a more resistive diesel to a more conductive microbial activity. The conductive temporal resistivity image suggested free phase diesel was removed and bioremediation was occurring as indicated by significant increases in conductance in the area found to be impacted by diesel and measure as highly resistive. CO2 measurements from the nearby wells confirmed the interpretation (Figure 5). Well samples were nondetect for diesel as of June 2017.

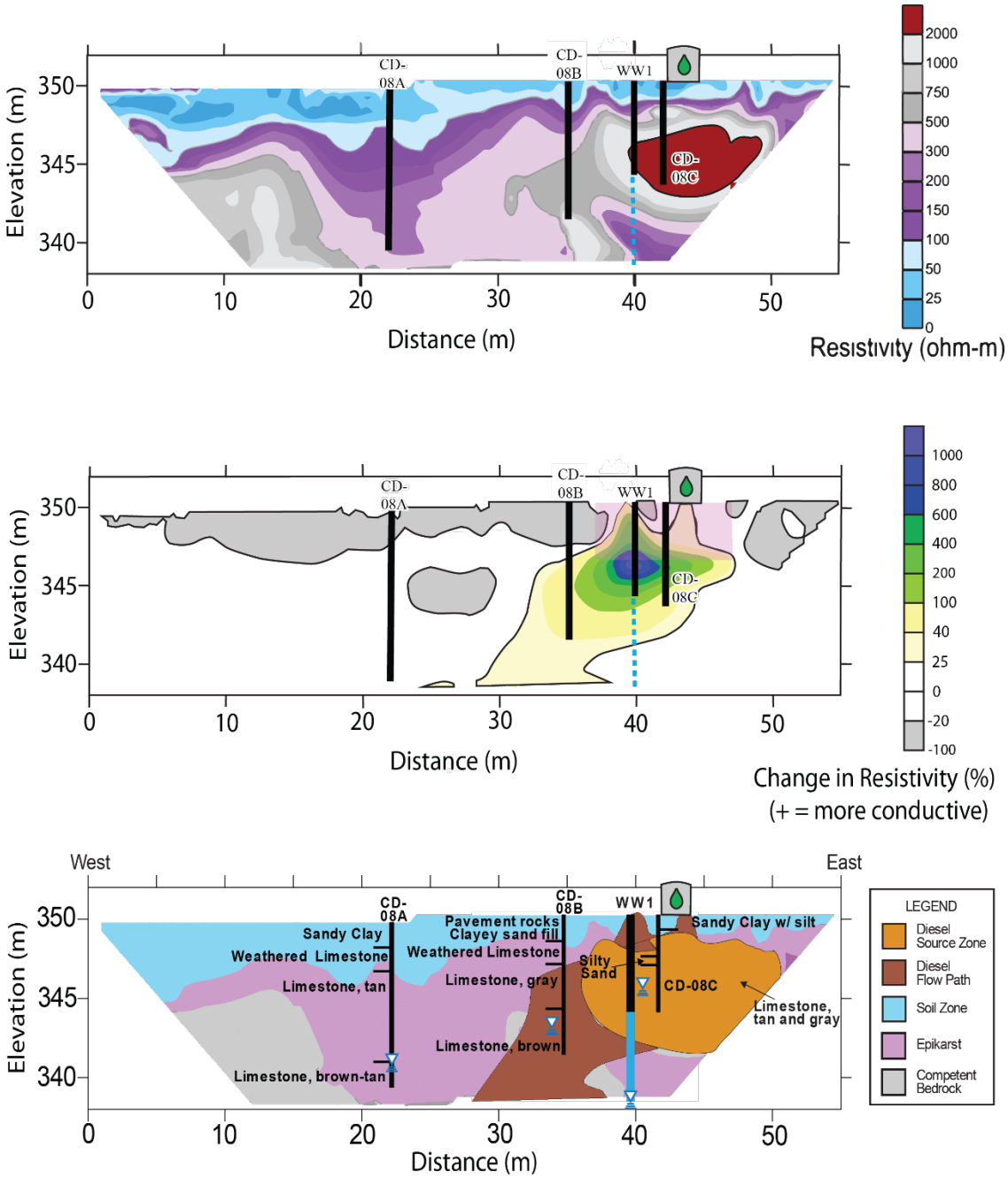

Figure 5: Development of a conceptual model using electric resistivity and drilling. 1) Shows the ERI before remediation; 2) Shows the ERI after remediation with bioremediation occurring and conductivity difference from 1; 3) Shows the conceptual model after applying ERI 1 and 2.

REMEDIATION

A total of 9 remediation technologies and methods were utilized at the site (Greystone Environmental et al., 2016a; Greystone Environmental et al., 2016b). The remediation techniques are broken into three categories: initial, active, and natural attenuation. Each category will have its own abbreviation followed by the number that pertains to which method it belongs to when it occurred. For example, evaporation is under the initial category and first to occur after the spill, so will be labeled I1.

Initial remediation methods occurred immediately after the spill and prior to site characterization. This included evaporation (I1) and excavation (I2). Evaporation occurred during the spill, before the diesel infiltrated the soil. Excavation was the first active remedial approach to remove source material. Evaporation occurred during the release of the contaminant as it flowed from the source and during infiltration. Excavation occurred on April 21, 2015 (Greystone Environmental et al., 2016a).

Active remediation consists of a range of commonly utilized remedial technologies. This category is split into pre-surfactant and post-surfactant remediation, as surfactant remediation changes certain site transport parameters after its use. Remedial technologies prior to surfactant flushing is submersible pump-and-treat (A1), skimmer pump-and-treat (A2) and soil vapor extraction (SVE) (A3). Post-surfactant flushing remedial technologies include skimmer pump-and-treat (A4) and SVE (A5). On September 15, 2015, skimmer pump-and-treat replaced submersible pump-and-treat in WW1. The skimmer pump was removed May 15, 2016 (Greystone Environmental et al., 2016a; Greystone Environmental et al., 2016b). Three separate soil vapor extraction events

occurred during remediation. The three events occurred from December 14-17, 2015, January 13-16, and January 17-29, 2016. Surfactant flushing and extraction began on March 28, 2016, with the installation of RW 1-3 and I1&I2. On April 1, 2016, pits for surfactant were excavated and surfactant flushing began. Soil vapor extraction and skimmer pump-and-treat remediation began starting on April 5, 2016.

More surfactant recovery continued on April 8, May 10-11, June 1, July 28, August 31, and ended on October 6, 2016 (Greystone Environmental et al., 2016a; Greystone Environmental et al., 2016b). On December 16, 2016, a temporal resistivity dataset was collected to correspond with the original ERI line ADA-08 to determine the effectiveness of remediation. WW1 was recompleted with 150 ft of steel surface casing (Greystone Environmental et al., 2016b). Monitoring wells at the site were sampled as non-detect for diesel as of June 2017.

Natural attenuation is natural degradation of diesel by either volatilization or by being utilized as a food source for microbes in the subsurface. Two natural attenuation methods were observed: volatilization (NA1) and bioremediation (NA2). It is also important to note that volatilization and bioremediation were enhanced after SVE use, but were still occurring prior or after use of SVE and other remedial technologies (Greystone Environmental et al., 2016b). The surfactant flush was noted to limit biodegradation for 2 months after it was applied as indicated by a decrease in the amount of carbon dioxide off gassing (Greystone Environmental et al., 2016b).

CHAPTER V

METHODS

This section describes the methodology for obtaining transport parameters from the site and for predicting mass removal of diesel using selected analytical models. First, the analysis of mass recovery from the field data collected during remediation is described for verification data. Then, the parameters used in mass removal modeling are described for each model. The methods for both sections follow in the order of the nine analytical models described in the previous section.

FIELD MEASURMENTS

INITIAL MASS RECOVERY

1) EVAPORATION: I1

Evaporation field measurements have no exact methodology and are difficult to obtain in field settings. Diesel evaporates quickly at first as the more volatile compounds dissipate but less volatile compounds are left behind (Fingas, 2013). When the diesel evaporation rate is plotted over time, the evaporation rate follows a square root function (Fingas, 2013). The diesel is estimated as 10% evaporated or approximately 760 L or 636 kg (200 gal or 1402 lbs) (Greystone Environmental et al., 2016a).

2) EXCAVATION: I2

The field method used for excavation is developed from the Oklahoma Department of Environmental Quality (Oklahoma Department of Environmental Quality, 2012). Soil is excavated onto a 10 mm (0.40 in) plastic sheeting, covered with a 10 mm (0.40 in) plastic sheeting, and a berm constructed around the pile to prevent rain water run-off (Greystone Environmental, 2016a). Each truckload is sampled with two scoops of a clean hand trowel into a clean 19 L (5 gal) bucket with a lid. Every tenth truckload, the samples are mixed and placed in a bag for laboratory analysis. The sampling method continues until the entire stockpile has been sampled. Each truck is weighed before and after dumping to record soil weights. Soil concentrations from the excavated pile is from the EPA laboratory method SM 2540G for total percent solids and method TNRCC 1005 for total petroleum hydrocarbons (TPH) range (American Public Health Association et al., 1998; Texas Natural Resource Conservation Commission (TNRCC), 2001; Greystone Environmental et al., 2016a). The estimated volume of diesel removed from field excavation is 1135 L or 950 kg (300 gal or 2094 lbs) (Greystone Environmental et al., 2016a).

ACTIVE MASS RECOVERY

3) SUBMERSIBLE PUMP-AND-TREAT: A1

The field method for mass estimation of submersible pump-and-treat remediation consisted of using a submersible 2.54 cm (4 in) pump at the depth to the water table surface and adjusted during pumping (Greystone Environmental et al., 2016a). The water and diesel mixture was pumped into above ground storage containers and were sampled by using EPA laboratory methods 8021 and 8000/8100 (U. S. EPA, 1982). The EPA laboratory method 8021 was used for

benzene, toluene, ethylbenzene, and total xylene (BTEX constituents). EPA method 8000/8100 was used for TPH and Diesel Range Organics (DRO). Diesel recovered is estimated to be 3220 L or 2695 kg (850 gal or 5942 lbs) (Greystone Environmental et al., 2016b).

4) SKIMMER PUMP-AND-TREAT: A2

The field method for skimmer pump-and-treat utilized a solar powered hydrophobic pneumatic skimmer pump once the free product thickness was less than 30.5 cm (1 ft) (Greystone Environmental et al., 2016a). The diesel was pumped directly into 1890 L (500 gal) tanks and removed from the site. Estimated field values were determined by measuring the amount of diesel fluid in the tanks. The amount of diesel removed from skimmer pump-and-treat method is estimated to be 2080 L or 1741 kg (550 gal or 3838 lbs) (Greystone Environmental et al., 2016a).

5) SOIL VAPOR EXTRACTION: A3

The field methodology for SVE consisted of using a Mini RAE portable photoionization detector (PID), that was calibrated with isopropane to measure estimated diesel vapor concentrations; a hi-vacuum Kinney Tuthill® liquid ring pump with 98 kPa (14 psi), 8.5 m^3/min (300 cfm); and a 7874 L (2080 gallon) tank and a 2.5 cm (1 in) drop tube placed on top of the remediation wells or down in WW1 to remove diesel (Greystone Environmental et al., 2016a). The PID measured hexane before and after SVE events to determine related diesel contamination. A Mini Rae 3000 measured PID, and a Mini Rae 3000 and RKI Eagle was able to measure CO_2 concentrations from the well and during SVE to estimate vapor concentrations and bioremediation. Estimated diesel removal through SVE is estimated to be 330 L or 276 kg (86.5 gal or 609 lbs) (Greystone Environmental et al., 2016a).

6) SURFACTANT ENHANCED SKIMMER PUMP-AND-TREAT: A4

The surfactant flushing field method included drilling surfactant recovery wells (RW1, RW2, and RW3), injection wells (I1 and I2), and excavating soil for three trenches around the site (Fig. 5) (Greystone Environmental et al., 2016b). The surfactant was mixed to the company and EPA recommendation of 3% surfactant in a 7571 L (2000 gal) water mixture. The surfactant was then gravity fed into the injection wells and trenches. An 1893 L (500 gal) aqueous injection, using a gravity feed method and a sprinkler system to simulate rainfall around the site was performed (Greystone Environmental et al., 2016b).

A skimmer pump was then installed into WW1 and skimmed during the SVE event. The surfactant and diesel mixture was pumped into removable above ground storage tanks and field values were measured by using the volume of diesel and surfactant in the tanks. The post-surfactant skimmer pump-and-treat is estimated to remove 23 L or 19 kg (6 gal or 42 lbs) of diesel (Greystone Environmental et al., 2016b).

7) SURFACTANT ENHANCED SOIL VAPOR EXTRACTION: A5

The Mini RAE portable photoionization detector was used before and after post-surfactant SVE events. The detector was calibrated with isopropane. A hi-vacuum Kinney Tuthill® liquid ring pump with 98 kPa (14 psi), 8.5 m^3/min (300 cfm); a 7874 L (2080 gallon) tank; and a 2.5 cm (1 in) drop tube was placed on top of the remediation wells, or down in WW1, to remove diesel (Greystone Environmental et al., 2016a). The PID measured hexane to determine the approximant amount of hydrocarbon removed after the post-surfactant SVE events. CO_2 was measured by a Mini Rae 3000 and RKI Eagle to determine the concentration during the SVE events.

Approximately 8 L or 7 kg (2 gal or 15 lbs) of equivalent hydrocarbon vapors were removed (Greystone Environmental et al., 2016a).

NATURAL ATTENUATION MASS RECOVERY

8) VOLATILIZATION ESTIMATION: NA1

Diesel has a low volatilization rate and the process was not considered during field remediation. No field values were estimated for this process, as it is difficult to measure in field settings; studies using soil columns demonstrated less than 4% of total loss of diesel concentration through volatilization (Møller et al., 1996). With an estimated 22.7 L (6 gal) of diesel remaining after the previous remedial methods, it is assumed less than 3.79 L or 3 kg (1 gal or 7 lbs) of diesel volatilized during remediation as volatilization can remove up to 36% of diesel in 230 days (Kroening et al., 2001).

9) BIOREMEDIATION: NA2

While McCoy (2012) used traps to capture CO_2 moving through the soil from bioactivity, CO_2 traps were not used at the study site as bioremediation was a side effect of SVE treatments and not in the remedial plan for the site (Greystone Environmental et al., 2016a; Greystone Environmental et al., 2016b). To measure estimated bioactivity in the field, the Mini Rae 3000 and RKI Eagle measured different concentrations of CO_2 during the remediation period and recorded the concentrations before and after remediation events (Greystone Environmental et al., 2016a). Field value is estimated for the remaining diesel of approximately 15.1 L or 13 kg (4 gal or 28 lbs) after the majority of mass is removed from the previous remedial methods and applying

the remainder diesel mass to bioremediation. Previous studies have shown up to 80% of diesel have been consumed in a four-week incubation period (Speight and Arjoon, 2012).

MASS RECOVERY MODELING

INITIAL MASS RECOVERY

1) EVAPORATION: I1

For evaporation modeling, the time to drain diesel from the two 3785 L (1000 gal) above ground storage tanks was calculated. The tank dimensions were taken from the Ada Characterization Report (2016a). Temperature data for the Fingas empirical evaporation equation was taken from the Fittstown Mesonet station online database (Brock et al, 1995; McPherson et al., 2007).

The horizontal tank drainage time equation was used to estimate the amount of time it took to gravity drain 7570 L (2000 gal). The equation is:

$$t = \frac{4L}{3C_d a\sqrt{2g}}\left[(2R - H_2)^{\frac{3}{2}} - (2R - H_1)^{\frac{3}{2}}\right], \quad (5.1)$$

where t is the time to drain the tank (s), L is the length of the tank (3.2 m or 10.5 ft), C_d is the coefficient of discharge (1.0), a is the area of the orifice (2.9×10^{-4} m^2 or 3.1 x 10^{-3} ft), g is the gravity constant (9.81 m^2/s or 32.17 ft^2/s), R is the radius of the tank (0.6 m or 2 ft), H_1 is the initial height of the liquid in the tank (1.2 m or 4 ft), and H_2 is the final height of the liquid in the tank (0 m or 0 ft) (Kunz, 2011). This time was used for equation (2.1). The estimated time to drain 7570 L (2000 gal) from the tanks was 155 min. As the spill occurred during a temperature transition from winter to early spring and the time of the spill is unknown over a three-month

period, temperature during the spill may be at lower or higher temperatures. Instead, the lowest, highest, and average temperature from when the tank was filled to when the spill was discovered was used. Since the time was only 155 min, temperature changes are small in this period. A constant minimum, maximum and average temperature was used during the 155 min interval. The temperature was used as the temperature value in equation (2.1). The minimum temperature was -10° C or 14° F (Brock et al, 1995; McPherson et al., 2007). The maximum temperature is 29° C or 84.2° F and the average temperature is 9° C or 48.2° F (Brock et al, 1995; McPherson et al., 2007).

2) EXCAVATION: I2

The data used for excavation came from the Ada Characterization Report (2016a). The data include the total weight of solids removed and sample concentrations. The samples were composited to calculate an average soil concentration. Calculated concentration of the soil was 1272 mg/kg using composite sampling methods.(Greystone Environmental et al., 2016a). Standard deviation for composited sampling was 1498 mg/kg. The standard error from calculated average was 387 mg/kg.

The excavation encountered competent bedrock at varied depths (Greystone Environmental et al., 2016a). The depth of the excavation was estimated with a minimum, maximum and best estimate from the various depths observed at the excavation. Minimum depth was estimated to be 1.8 m (6 ft). Maximum pit depth was estimated to be 3.0 m (10 ft). The average depth of the pit was 2.4 m (8 ft). The spatial extent of the excavation is also not a simple geometrical shape (Figure 4). Like the depth, the area varied with an estimated minimum, maximum and best-estimated area.

Minimum excavated area is 133 m^2 (1432 ft^2) (Greystone Environmental et al., 2016a). Maximum excavated area is 185 m^2 (1991 ft^2) (Greystone Environmental et al., 2016a). The best-estimated area is 151 m^2 (1625 ft^2) (Greystone Environmental et al., 2016a).

Additional data used for the model was the density of diesel and the density of the dolomite bedrock. The average density of diesel used was 0.83 kg/m^3 (Song et al., 2000). The density of the dolomite bedrock was not measured from the field and the average density of 2.63 kg/m^3 was used as the density of dolomite bedrock range from 2.5 to 2.8 kg/m^3 (Manger, 1963).

ACTIVE MASS RECOVERY

3) SUBMERSIBLE PUMP-AND-TREAT: A1

The parameters for inputting the initial depth intervals, LNAPL properties, and soil properties are from the Ada Characterization Report (2016a) or literature values such as Charbeneau (2003) or Environmental Canada (2014). API LDRM calculates equations (2.3) through equations (2.20) at twenty equally distributed intervals from lower water saturated thickness to maximum LNAPL thickness (Charbeneau, 2007). Some of the parameters for submersible pump-and-treat inputs are known and have a constant value. The time of recovery is 79 days (Greystone Environmental et al., 2016a; Greystone Environmental et al., 2016b), the well radius of the predicting well is 0.51 m (20 in) (Greystone Environmental et al., 2016a; Greystone Environmental et al., 2016b), the radius of influence is 132 m (433 ft) (Pickens and Halihan, 2016), and saturated thickness or groundwater thickness is 286 m (938 ft) (Christenson et al., 2011).

The variable parameters are the pumping rates and the radius of capture. The water pump installed was designed to pump no more than 37.9 L/min (10 gpm) to reduce the risk of smearing. Minimum and maximum water production rates were 18.9 L/min (5 gpm) and 37.9 L/min (10 gpm). Estimated water production rate is 26.5 L/min (7 gpm). The radius of capture is determined from using similar minimum, maximum and best-estimated values shown in a skimmer pump-and-treat radius (Charbeneau, 2007). Minimum radius of capture is approximately 3.05 m (10 ft), maximum radius of capture is estimated to be 7.62 m (25 ft), and an average radius of capture is 5.30 m (17 ft).

4) SKIMMER PUMP-AND-TREAT: A2

Data for inputting the initial depth intervals, LNAPL properties, and soil properties were obtained from the Ada Characterization Report (2016a) and several literature values such as Charbeneau (2003) and Environmental Canada (2014). API LDRM was used for skimmer pump-and-treat prediction. The inputs were the same for soil and diesel properties from the submersible pump-and-treat method.

Several equations from the submersible pump-and-treat are used for the skimmer pump-and-treat. Equation (2.3) to equation (2.6) and equations (2.8) to equation (2.9) are used in calculation of skimmer pump-and-treat. However, the skimmer pump-and-treat method in the API LDRM calculator uses equation (2.13) through equation (2.17) for calculation. It also requires the selection of whether the aquifer is unconfined, confined, or perched (Charbeneau, 2014). The aquifer type changes the LNAPL thickness and possible soil interval. If the aquifer is unconfined, LNAPL thickness equation is:

$$b_{nW} = \frac{z_{wt} - z_{12}}{\rho_r}, \quad (5.2)$$

Where b_{nW} is the LNAPL thickness in the well constrained by fine-grain zone (Charbeneau, 2014).

If the aquifer is confined, the model assumes the upper soil facies is the confining layer at the water table is above the soil interface (Charbeneau, 2014). The LNAPL thickness is calculated using:

$$b_{nW} = \frac{z_{wt} - z_{12}}{\rho_r}, \quad (5.3)$$

Where z_{wt} is the elevation of the water table, z_{12} is the elevation of the interval between soil 1 and soil 2 (Charbeneau, 2014).

If the aquifer is perched, the model assumes the bottom soil layer is the perching layer and the water table is located below the soil interface (Charbeneau, 2014). The LNAPL thickness is modified using the equation:

$$b_{nW} = \frac{z_{12} - z_{wt}}{(1 - \rho_r)}, \quad (5.4)$$

(Charbeneau, 2014). Where equations (5.2), (5.3), and (5.4) are used in equations with the parameter b_{nw} to adjust for the aquifer type. Initial soil thicknesses, water table depths, LNAPL parameters, and soil parameters are the same as submersible pump-and-treat. The LNAPL thickness changes after previous remediation from the pump-and-treat. Known parameters that will not vary are time, well radius, and aquifer conditions. The time for skimmer pump-and-treat recovery is 129 days (Greystone Environmental et al., 2016a; Greystone Environmental et al., 2016b) and well radius is 0.51 m (20 in) (Greystone Environmental et al., 2016a). While the

aquifer is geologically a confined aquifer, the water table was deep enough during this time that it did not cross the simulated second and third "soil" intervals. An unconfined aquifer was used for the model to work correctly.

The only parameters that were unknown from the field was the radius of capture. However, other field studies have shown the radius of capture ranges from 3.0-150 m (9.8-492 ft) (Charbeneau, 2007). At the site, skimmer pumping rates were equivalent to the rates of submersible pumping, equaling the same radius of capture. The minimum radius of capture is assumed to be 3.05 m (10 ft). The maximum radius of capture is assumed to be 7.62 m (25 ft) as the pumping rate is no more than 38 L/min (10 gpm) and the radius of capture will be smaller than 150 m (492 ft). The average radius of capture is 5.3 m (17 ft).

5) SOIL VAPOR EXTRACTION: A3

Data used for SVE removal models includes site data from the Ada Characterization Report (2016a), the Ada Surfactant Report (2016b). Additional site specific data were available from the United States Department of Agriculture: Natural Resources Conservation Service (USDA: NRCS) (Soil Survey Staff et al., 2016). Several literature sources for contaminant values such as Fogg (1990) for molecular weight and vapor pressure, Brock et al. (1995), McPherson et al. (2007) for Mesonet temperature data, and Johnson et al. (1990) for suggested radius of influence and well pressure values were also utilized.

Initial diesel vapor concentrations are calculated by using equation (2.19), which uses molecular weight, vapor pressure, temperature, and the gas constant. The molecular weight for diesel is estimated to be 234 g/mol (Fogg, 2017). The vapor pressure of diesel is estimated to be 2.03 kPa

(0.29 psi) (Fogg, 2017). The temperature in the subsurface is estimated to be 293 K (67.7° F) (Brock et al., 1995; McPherson et al., 2007).

Equations (2.19) and (2.22) calculates a single SVE well and not multiple SVE wells. Each SVE well was calculated with corresponding well screen lengths, then totaled to determine the value of diesel vapor removed. The well screen length used is the total screen length assuming there is no water or liquid diesel in the well. The consistent values used are flow rates (Q), viscosity of air (μ), absolute ambient pressure (P_{atm}), radius of the extraction wells (R_w) and well screen lengths (H). The flow rate is 0.142 m^3/s (301 cfm) (Greystone Environmental et al., 2016a; Greystone Environmental, 2016b). The viscosity of air is 1.8×10^{-4} g/cm·s (1.2×10^{-5} lbs/ft·s) (Johnson et al., 1990). Absolute ambient pressure is 1.01×10^{6} g/cm (6.8×10^{4} lbs/ft) (Johnson et al., 1990). Radius of the extraction wells CD-8b, CD-8c, CD-8d, CD-8e, and CD-8f is 0.051 m (2 in) (Greystone Environmental et al., 2016a; Greystone Environmental, 2016b). The well screen lengths for CD-8b and CD-8c is 1.5 m (5 ft) and well screen lengths for CD-8d, CD-8e, and CD-8f is 9.1 m (30 ft) (Greystone Environmental et al., 2016a; Greystone Environmental, 2016b).

The absolute pressure of the wells varied during pumping for SVE. A constant minimum, maximum and average pressure of SVE values from field studies were used. Minimum absolute pressure at the extraction wells was 96.3 kPa (14.0 psi) (Johnson, 1990). Maximum absolute pressure at the extraction wells was 91.2 kPa (13.2 psi) (Johnson, 1990). Average absolute extraction well pressure was 94.2 kPa (13.7 psi) (Johnson, 1990). Radius of influence also varied for SVE. Minimum, maximum, and the average radius of influence were taken from literature values. Minimum SVE radius of influence was 9.0 m (29.5 ft) (Johnson, 1990). Maximum radius of influence for SVE wells was 16.0 m (52.5 ft) (Johnson, 1990). Average radius of influence for

each extraction well was 12.0 m (39.4 ft) (Johnson, 1990). Permeability of the soil was not determined but equation (2.20) can be rearranged to calculate permeability (Calabrese and Kostecki, 1992). Using the values and data from the Ada Characterization Report (2016a) and Ada Surfactant Report (2016b), it can be calculated using the equation:

$$k = \frac{Q\mu}{H\pi p_w \frac{[1-(P_{atm}/P_w)^2]}{\ln(R_w/R_I)}}, \tag{5.5}$$

(Calabrese and Kostecki, 1992). The minimum, maximum, and average absolute pressure and radius of influence for each well to calculate minimum, maximum, and average permeability of the soil for each SVE extraction well. The calculated minimum permeability is 3.6 x 10^{-11} m^2 (3.9 x 10^{-10} ft^2). The calculated maximum permeability is 1.1 x 10^{-10} m^2 (1.2 x 10^{-9} ft^2). The average permeability is calculated to be 7.2 x 10^{-11} m^2 (7.8 x 10^{-10} ft^2).

6) SURFACTANT ENHANCED SKIMMER PUMP-AND-TREAT: A4

Field data from the post-surfactant skimmer pump-and-treat remediation was obtained from the Ada Surfactant Report (2016b). The post-surfactant skimmer pump-and-treat model uses the same equations and methodology as the pre-surfactant skimmer pump-and-treat model for saturation and recovery. Constant parameters are time, well radius, depth to water table, soil properties. Most LNAPL properties are the same except LNAPL thickness and interfacial oil/water tension, which were adjusted for the post-surfactant phase. The time of pumping is approximately 28 days (Greystone Environmental et al., 2016b).

Variable parameters are the radius of capture and interfacial oil/water tension. Radius of capture was the same as model A2: Skimmer Pump-and-Treat. Interfacial oil/water tension for diesel was

similar around 24.1 dyne/cm (1.4 x 10^{-4} lbs/in) (Canada Environmental, 2014). However, with the application of surfactants, it can decrease three orders of magnitude degrees (Martel and Gélinas, 1996). Diesel/water tension has been observed to decrease with rhodamine dye (Martel and Gélinas, 1996). The minimum decrease of oil/water tension was 19.4 dyne/cm (1.1 x 10^{-4} lbs/in) (Martel and Gélinas, 1996). Maximum of interfacial tension decrease was 0.241 dyne/cm (1.4 x 10^{-6} lbs/in). Average decrease of interfacial oil/water tension was 2.41 dyne/cm (1.4 x 10^{-5} lbs/in).

7) SURFACTANT ENHANCED SOIL VAPOR EXTRACTION: A5

Data used for the post-surfactant SVE model comes from the Ada Surfactant Report (2016b). Initial diesel vapor concentrations were calculated using the same method and values as for model A3: SVE. Flow rates for the model also used the similar method of calculating flow rates for each well and totaling them for a sum of vapor extraction. The varied permeability was calculated the same as for a well using the post-surfactant SVE data for the reduced permeability values.

SUBSURFACE PARAMETERS

The following are the parameters used for both submersible and skimmer pump-and-treat models using the LDRM. For the subsurface section of the LDRM inputs, different LNAPL thickness was used for models A1, A2, and A4. The LNAPL thickness for the submersible pump-and-treat model was 0.762 m (2.5 ft) (Greystone Environmental et al., 2016b). LNAPL thickness for the skimmer pump-and-treat models for pre-surfactant was 0.305 m (1.0 ft) and post-surfactant was 0.024 m (0.079 ft) (Greystone Environmental et al., 2016a; Greystone Environmental et al., 2016b).

	Layer 1	Layer 2	Layer 3	Source
Porosity (n) – unitless	0.41	0.46	0.15	Charbeneau, 2003; Christenson et al., 2011
Hydraulic Conductivity (K_{ws}) m/d	3.35	0.001	4.96	Charbeneau, 2003; Pickens and Halihan, 2016
Van Genuchten "N" unitless	2.28	1.37	2.00	Gerke and van Genuchten, 1993; Charbeneau, 2003
Van Genuchten "α" m^{-1}	12.5	1.61	10.0	Gerke and van Genuchten, 1993; Charbeneau, 2003
Irreducible Water Saturation (S_{wr}) - unitless	0.41	0.034	0.43	Charbeneau, 2003
Residual LNAPL Saturation (S_{ni}) - unitless	0.50	0.63	0.15	Charbeneau, 2003

Table 3: Properties for each soil layer used in the API LDRM

Ground surface elevation was selected for zero. Water table depth used was 26.2 m (86 ft) (Greystone Environmental et al., 2016b). The vertical hydraulic gradient was treated as zero as the observation well was also the extraction well.

For model LNAPL parameters, density, viscosity, air/LNAPL surfacial tension, and water/LNAPL interfacial tension was taken from Environmental Canada Diesel Properties Report (2011). Density of diesel was 0.83 kg/m3 (Environment Canada, 2017). Viscosity was 0.002 Pa·s (Environment Canada, 2017). Air/LNAPL surfacial tension was 27.3 dyne/cm (1.6 x 10-4 lbs/in) and water LNAPL interfacial tension prior to surfactant use was 24.1 dyne/cm (1.4 x 10-4 lbs/in) (Environment Canada, 2017).

The relative permeability models selected were the Burdine and Mualem models. The Burdine model assumes the material is coarse grain while the Mualem model assumes the media is fine-grained. Layer 1 was the coarsest material in the subsurface and the Burdine model was selected. Layers 2 and 3 were considered fine-grained material and use the Mualem model (Table 2). Soil parameters for all three model layers included porosity, hydraulic conductivity, van Genuchten "N" and "α" parameter, irreducible water saturation, residual LNAPL saturation and f-factor (Table 2). Residual LNAPL f-factors for model soil layers 1, 2, and 3 were not selected for the model.

NATURAL ATTENUATION MASS RECOVERY

8) VOLATILIZATION: NA1

The Hamaker equation (2.38) requires a initial vapor concentration, a total area of the diesel plume in the subsurface and how long volatilization has occurred. Estimation of the volatilization rate of diesel used the initial vapor concentration equation (Equation 2.19) that SVE initially used. This used the same initial diesel vapor concentration value in the SVE: A2 model.A minimum, maximum, and average area used in equation (2.22) was measured from the Ada Characterization Report (2016a) and Ada Surfactant Report (2016b). The minimum area was 18 m^2 (194 ft^2), the maximum area was 35 m^2 (377 ft^2), and the average area was 70 m^2 (753 ft^2). The time of volatilization occurring at the site was from the time the initial spill was discovered to when non-detect was reported. The time of the discovery of the spill to the site reporting non-detects was approximately 2 years (Greystone Environmental et al., 2016a; Greystone Environmental et al., 2016b).

9) BIOREMEDIATION: NA2

Data used for the estimation of mass removal via bioremediation was from the Ada Characterization Report and Ada Surfactant Report (Greystone Environmental et al., 2016a; Greystone Environmental, 2016b). CO_2 measurements were taken from the multi-gas infrared detector taken at various times at each well at the site before and after the application of remedial activities. For estimated mass removal rates, the concentration of CO_2 measured from the field was converted into a flux in units of $\mu mol/m^2/s$. The CO_2 flux rate was converted from $\mu mol/m^2/s$ to L/acre/yr using McCoy's stoichiometric conversion using an equivalent organic compound (McCoy et al., 2012). McCoy selected decane ($C_{10}H_{22}$) for stoichiometric conversion for gasoline. Diesel has higher concentration of organic compounds heavier than decane; this may not accurately provide mass removal of diesel via bioremediation. Instead, minimum, maximum, and average equivalent organic compounds were used. Minimum equivalent organic compound was decane as it was a basis for McCoy's method. Maximum equivalent organic compound was hexadecane ($C_{16}H_{34}$), due to it being used in multiple studies in biodegradation (Wodzinski and Johnson, 1968; Geerdink et al., 1996; Roy and Greer, 2000; Krummenacher et al., 2003). The average equivalent organic compound was cyclododecene ($C_{12}H_{22}$) as the average between decane and hexadecane.

MODEL UNCERTAINTY EVALUATIONS

The analytical model results were compared to values retrieved from the site to determine the error in model estimates. Some of the remedial methods have quantitative values to compare from the field. Quantitative values include excavation (I1), submersible pump-and-treat (A1), skimmer

pump-and-treat (A2 & A4), and SVE (A3 & A5). The other methods, evaporation (I2), volatilization (NA1) and bioremediation (NA2) have no quantitative values to compare to either due to difficulty of field measurements or no remedial plan to measure mass removal rates for that method.

CHAPTER VI

RESULTS

This section details the results from the mass removal models compiled in Chapter III and using the parameters provided in Chapter IV. The mass removal and model uncertainty for each individual model are presented (Figure 6). The mass removal contribution of each remedial method relative to the known total mass is also presented (Figure 7). The results are detailed in the same order as the previous sections.

INITIAL MASS RECOVERY

1) EVAPORATION: I1

The evaporation model with minimum values for parameters predicted 251 L (66 gal) or 210 kg (463 lbs) of diesel would evaporate. The evaporation model with average values predicted 482 L (127 gal) or 403 kg (889 lbs.), and the maximum values predicted 727 L (192 gal) or 210 kg (463 lbs.) would evaporate. This is a range of 3% to 10% of the mass with an average model estimate of 6%.

Of the 7571 L (2000 gal) spilled at the site, 757 L (200 gal) or 634 kg (1397 lbs.) or 10% of diesel was removed through evaporation as the field estimate. The estimated error of field amount was 10%. The evaporation model generally under predicted the field estimate. The range of under prediction was 4% for the maximum model parameters and 67% for the minimum. The difference between the field amount and the average model prediction was 36%.

2) EXCAVATION: I2

The excavation model with minimum values for parameters predicted 1047 L (276 gal) or 876 kg (1932 lbs.) of diesel would be removed with the soil and weathered dolomite. The excavation model with average parameter values predicted 1575 L (416 gal) 1318 kg (2906 lbs.) with maximum values of 2414 L (638 gal) or 2021 kg (4454 lbs.) of diesel. This resulted in a range of mass removal between 14% and 32% of the 7571 L (2000 gal) spill. The average excavation model estimate anticipated a 21% removal.

The field data suggested that of the 7571 L (2000 gal) spilled at the site, 1170 L (300 gal) or 979 kg (2159 lbs.) or 15% of diesel was removed through excavation. Estimated error of the field calculation was 30%. The difference between the field measurement and minimum model prediction was an 8% model under prediction. The average model and the maximum model predictions over predicted the field measurement by 39% and 113%. The range of model results for excavation are consistent with the field data with a general over prediction based on the average model estimate.

ACTIVE MASS RECOVERY

3) SUBMERSIBLE PUMP-AND-TREAT: A1

The API LDRM code with minimum values for parameters predicted 644 L (170 gal) or 539 kg (1188 lbs.) of diesel would be removed. The prediction with average values was 1156L (305 gal) or 968 kg (2133 lbs.), and with maximum values, 1376 L (364 gal) or 1152 kg (2539 lbs.) of diesel would be removed. Thus, the model predicted a removal of between 9% and 18% through

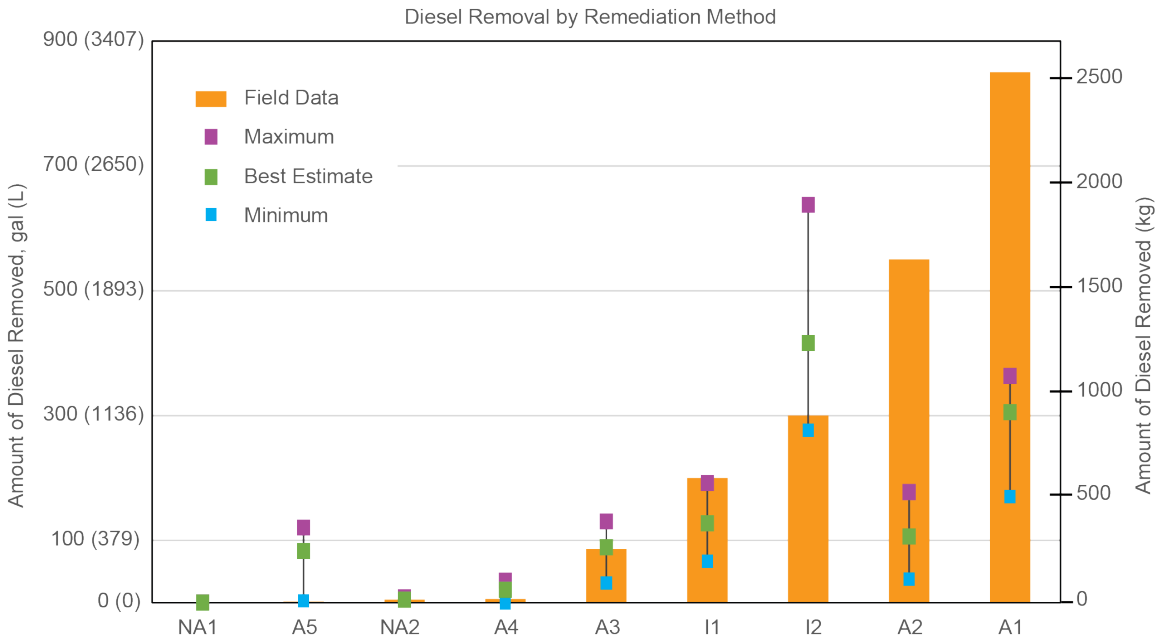

Figure 6: Model volume of diesel mass removed for each remedial method (squares) versus the field estimate of diesel removed (blue bars) in order of lowest to highest field mass value

submersible pump-and-treat with an average model estimate of 15%.

Of the 7571 L (2000 gal) spilled at the site, 3217 L (850 gal) or 2639 kg (5936 lbs.) or 43% of diesel was removed through submersible pump-and-treat. The field measurement error was estimated to be 10%. The model significantly underestimated the amount of mass recovery through submersible pump-and-treat with an under prediction between 57% and 80%. The average values provided a model estimate that was 64% below the measured field value.

4) SKIMMER PUMP-AND-TREAT: A2

The API LDRM code with minimum values for parameters predicted 143 L (38 gal) or 120 kg (264 lbs.) of diesel would be removed via skimmer pump-and-treat. For average values, the model predicted 403 L (106 gal) or 337 kg (744 lbs.), and with maximum values the prediction

was 672 L (178 gal) or 562 kg (1240 lbs.). This results in estimates of mass removal between 2% and 9% with an average estimate of 5%.

Of the 7571 L (2000 gal) spilled at the site, a field estimate of 2082 L (550 gal) or 1743 kg (3842 lbs.) or 43% of diesel was removed through skimmer pump-and-treat. The field measurement error was estimated to be 10%. The model significantly under predicted mass removal for this method. The error between the field measurement and the model estimate was an under prediction between 68% and 93%. Using average values, the model under predicted by 81%.

5) SOIL VAPOR EXTRACTION: A3

The SVE model with minimum values for parameters predicted 121 L (32 gal) or 101 kg (223 lbs.) of diesel would be removed. The average values provided an estimate of 337 L (89 gal) or 282 kg (622 lbs.), and the SVE model with maximum values predicted 494 L (130 gal) or 413 kg (912 lbs.) of diesel would be removed. This would provide a range of 1% to 11% of the diesel impact. The average estimate from the model 366 would be 9% mass removal.

Of the 7571 L (2000 gal) spilled at the site, 327 L (86 gal) or 274 kg (603 lbs.) or 4% of diesel was removed through SVE. The estimated field measurement error was 10%. The model was in the range of the field measured value. The minimum model prediction under predicted by 63%, while the maximum model over predicted by 52%. The difference between the field estimate and the average model prediction is a 3% model over prediction. Overall, the model slightly over predicted the amount recovered compared to the field amount recovered.

6) SURFACTANT ENHANCED SKIMMER PUMP-AND-TREAT: A4

The API LDRM code with surfactant enhancements predicted 0.1 L (0.02 gal) or 0.1 kg (0.2 lbs.) of diesel would be removed via skimmer pump-and-treat using the minimum value estimates. The average parameters resulted in an estimate of 78 L (21 gal) or 65 kg (144 lbs.), and the maximum values for parameters predicted 136 L (36 gal) or 114 kg (251 lbs.) of diesel would be removed. This would be a range of 0.001% to 2% of the diesel impact. The average estimate from the model would be a removal of 1%.

Of the 7571 L (2000 gal) spilled at the site, 23 L (6 gal) or 19 kg (42 lbs.) or 0.3% of diesel was removed through surfactant enhanced skimmer pump-and-treat. The field error was estimated to be 10%. The model was within range of the field data, but generally over predicted. The difference between the field amount and the minimum model prediction was 100% model under prediction. The difference between the field amount and the maximum model prediction was 499% over prediction. The difference between the field amount and the average model prediction was 250% over prediction.

7) SURFACTANT ENHANCED SOIL VAPOR EXTRACTION: A5

The SVE model with surfactant enhancements with minimum parameter values predicted 12 L (3 gal) or 10 kg (22 lbs.) of diesel would be removed. Using average values, the prediction would be 314 L (83 gal) or 263 kg (579 lbs), and with maximum values, a predicted 457 L (121 gal) or 383 kg (843 lbs) of diesel would be removed. These values represent a range of 1% to 9% mass removal, with an average model estimate of 3%.

Of the 7571 L (2000 gal) spilled at the site, a field estimate of 8 L (2 gal) or 7 kg (15 lbs) or 0.1% of diesel was removed through SVE with surfactant enhancement. The field error was estimated

to be 10%. Overall, the model significantly over predicted the measure quantity from the field. The difference between the field amount and the minimum model prediction was a 59% over prediction. The difference between the field amount and the maximum model prediction was 5934% over prediction. The average model over prediction was 4045%.

NATURAL ATTENUATION

8) VOLATILIZATION: NA1

The volatilization model with minimum values for parameters predicted 0.96 L (0.25 gal) or 0.8 kg (1.8 lbs) of diesel would be removed. With average parameters the amount would be 1.9 L (0.49 gal) or 2 kg(4 lbs), and with maximum values the model predicted 3.7 L (0.98 gal) or 3 kg (7 lbs) of diesel would be removed. This represents a removal of between 0.003% and 0.005% of the diesel mass. The average parameters resulted in an estimate of 0.003% removal.

Of the 7571 L (2000 gal) spilled at the site, 4 L (1 gal) or 3 kg (7 lbs) or 0.05% of diesel was removed through volatilization. Estimated field error was 10%. The model estimates all under predicted the amount removed through volatilization. The under prediction ranged from 2% to 75% with an average value of 51%.

9) BIOREMEDIATION: NA2

The bioremediation model with minimum values for parameters predicted 15 L (4 gal) or 13 kg (28 lbs) of diesel would be removed without actively aiding any bioremediation process. Using average parameters, the amount predicted would be 19 L (5 gal) or 16 kg (35 lbs) and with maximum values, 34 L (9 gal) or 28 kg (63 lbs). These model estimates represent a mass removal

between 0.2% and 0.5% of the original mass. The average model estimate would be 0.3%.

Of the 7571 L (2000 gal) spilled at the site, a field estimate of 19 L (5 gal) or 16 kg (35 lbs) or 0.3% of diesel was removed through bioremediation. Estimated error of field values was 10%. The model and the field data agree fairly well. The difference between the field estimate and the minimum model prediction is a 19% under prediction. The difference between the field amount and the maximum model prediction is a 79% over prediction. The difference between field and the average model prediction is only a 0.21% under prediction. Overall, the model is in excellent agreement with the field estimate.

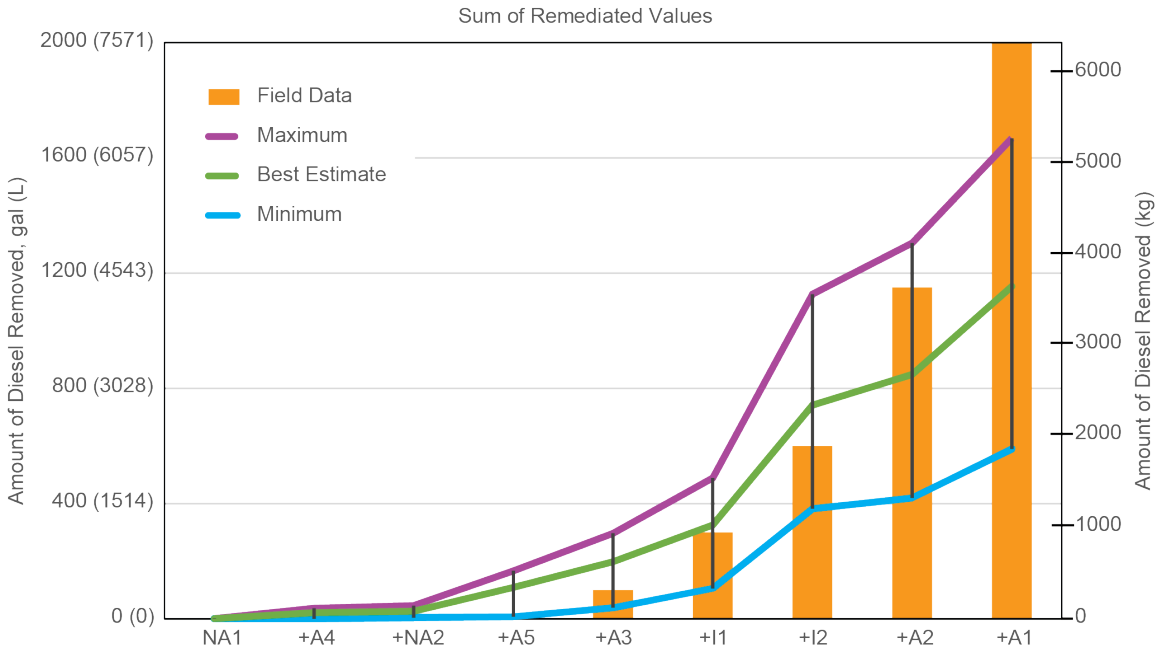

Figure 7: The sum diesel volume removed for each remedial model estimate in order from smallest to largest volume (colored lines) with minimum, average, and maximum estimates. The blue bars graph in order of smallest to largest volume the field estimates of volume removal of diesel for a site with known impacts and nondetect conditions post remediation.

CHAPTER VII

DISCUSSION

This section discusses the issues with parameter variability and estimation, model variability, possible error reduction, and future work to assist in hydrocarbon mass removal modeling. The models that were accurate within 10% of the average were SVE and bioremediation. Models that were moderately accurate within 11% to 60% of the average were excavation and evaporation. Models that did poorly, or greater than 60% of the average, were submersible pump-and-treat, skimmer pump-and-treat, surfactant enhanced skimmer pump-and-treat and surfactant enhanced SVE.

PARAMETER VARIABILITY AND ESTIMATION

Possible model uncertainties in the mass removal models were based on the variability of the parameters and best parameter estimations for selected models. Diesel physical properties such as density, interfacial tension, vapor pressure, and molecular weight vary due to crude oil origin, distillation methods, individual company mixtures, and diesel additives (Song et al., 1990; Fingas, 2001). Testing physical and chemical properties of diesel for density, interfacial tension, vapor pressure, and molecular weight could reduce uncertainties in prediction equations. Density can affect the results by 12% to 111%. Interfacial tension can affect the model results by less than 1% to 39%. Vapor pressure can affect the model results by 71%, and molecular weight can affect the model results by 17%. Although free product may exist on an impacted site, these parameters are not commonly measured, but could significantly affect the estimates of mass removal.

MODEL VARIABILITY

By necessity for simplified analytical models, the models rely on assumptions about flow and transport mechanisms. Models that calculate flow rely on several parameters that may not be well defined to calculate transport parameters that are assumed, ignored, or refer to previous studies. Most models don't account for any change of chemical composition during the remedial process or areas of influence that has little or no contaminants.

Evaporation does not calculate for infiltration into the soil, where temperatures in the soil are different from the atmosphere. Once the diesel infiltrates into the soil, it may begin to change from liquid to gas phase more readily than at colder surface conditions. This would likely not generate significantly different estimates for the total mass removal.

Excavation uses an average concentration over an entire excavated pit, when some zones of the pit may not be impacted. This would over predict the amount removed using equation (2.2). The equation is also simple making it sensitive to parameter variability as changing the density of diesel from 0.837 g/cm^3 to 0.800 g/cm^3 results in a decrease of 57% while an increase from 0.837 g/cm^3 to 0.860 g/cm^3 results in an increase of 59% (Song et al., 2000). Variation of pit volume ranges from 20% decrease and 21% increase from the average pit volume. The standard error for composite pit concentration of 387 mg/kg changes the excavation results by 13%. This is smaller than expected and suggests that compositing is a reasonable approach to get a good estimate for mass removal (U.S. EPA, 2002).

The API LDRM submersible pump-and-treat model may be underestimating due to the thickness of the saturated column. The model is assuming the saturated thickness is the same as the well

screened length. For Ada WW1, the screened length is about 300 m (984 ft) and the model is assuming the whole borehole is pumped at 26.5 L/min (7 gpm). While drawdown may adjust for water above the pump intake, it is unknown how much water is flowing beneath the pump intake caused by the pumping. This is unique for this site with a deep production well, and may not affect most sites where the methods are applied.

The API LDRM skimmer pump-and-treat model does not have an input for pumping rate; the pumping rate of LNAPL using a skimmer pump is calculated using equation (2.13). The pumping rate used in the field may be different than what LDRM calculates as the skimmer pump may be able to pump at higher or lower rate than calculated. Another issue is the LDRM skimmer pump-and-treat relies on the observation well for radius of capture. The model assumes the contaminated observational well equals the radius of capture. At the site, none the observational wells CD-03, CD-05, CD-06 were contaminated with diesel. The remediation well was also the observational well. This may affect the prediction of diesel removal as LNAPL head at the radius of capture equals the thickness of the LNAPL. The thickness of LNAPL may not fully extend to the radius of capture and may not be the same thickness throughout the radius of capture. This will either over predict or under predict the saturation and recoverable volume of LNAPL. An additional problem for both the API LDRM submersible pump-and-treat and skimmer pump-and-treat models may be the lack of dual permeability models for fractured and karstic aquifers.

Soil vapor extraction uncertainty is small but could be further reduced by measuring radius of influence, soil temperature, and vapor concentration before each SVE event.. Measuring the radius of influence will determine if SVE will reach the entire contaminated area. If the radius of influence covers the entire contaminated area and some uncontaminated area, Johnson et al.

(1990) provides a scenario where a fraction of vapor flows through uncontaminated soil. Soil temperature can be measured to reduce the SVE error as increasing the temperature can increase the vapor concentration (Johnson et al., 1990). The equations do not account for vapor compositional changes and mass transfer resistances during SVE. While equation (2.19) estimates the initial concentration, it can be measured before each SVE event to predict how much vapor each SVE event can remove.

Problems with the model prediction of skimmer pump-and-treat and SVE surfactant flushing include the wide variability of interfacial tension reduction and surfactants suppressing volatilization that SVE relies on. It can be difficult to determine if surfactant will not only reach the affected area, but also mobilize and solubilize the contaminant in the field. If it does, the degree of interfacial decrease varies depending on the concentration of the surfactant and soil. The API LDRM calculated the correct trend of increasing diesel recovered with decrease of interfacial tension but over predicted the field value. Surfactants can also suppress volatilization of the LNAPL (Chao et al., 2006; Chao et al., 2008) and equation (2.19) does not account for surfactant vapor suppression. This may be the reason values are so high for the minimum, maximum, and average values. The vapor concentration of the subsurface can be sampled to replace equation (2.19).

Another issue is the models do not interfere with each other nor account previous remedial efforts. If SVE was conducted before any pump-and-treat methods, the model does not account for liquid free product in the well. This could affect the length of the exposed well screen and may affect hydrocarbons located at the liquid-air boundary but not below the surface of the LNAPL. If SVE was not used, bioremediation may not have the same effect both in the field and

in analytical models. If the order of remedial methods were switched or no conducted at all, the models may predict either different values or not account the order of remediation methods.

FUTURE WORK

Future work includes more testing and average values of diesel composition parameters for a database or method to determine source parameters that vary with composition. Work could also be done to limit the conceptual uncertainties of the analytical models utilized. Additionally, the parameters of a biodegradable water based blend of non-ionic ethoxylated octylphenolic surfactant should be more precisely determined.

Diesel physical and chemical parameters are complex and vary based on reservoir source, oil distilling company procedures, distillation process, and additives (Song et al., 2000; Fingas, 2001). These factors may change the density, molecular weight, volatility, and other parameters used to calculate mass removal. A database of diesel parameters showing the variability from reservoir source, originating company, distillation process, and additives, may make modeling more precise.

Future for work for the analytical predictive models need recognition for API LDRM and evaporation. The API LDRM focus could be the effect of how much water is being pumped by a skimmer well for such a deep open borehole well. Not all 300 m (984 ft) of water could be flowing toward the pump to be extracted and may need to be adjusted for partially penetrating flow. Another possibility could be the use of van Genuchten equation with a fractured system. Gerke and van Genuchten developed a dual permeability model to determine the extent of saturation in a fractured matrix.

For evaporation, infiltration is not considered in the empirical equation (2.1). Infiltration rates could be found for different types of soil and added to empirical equation (2.1) as an additional empirical equation. Ma et al. (2016) has already determined diesel oil infiltration in fine sand and silty clay loam. Ma et al. (2016) also determined how soil texture, soil bulk density, and initial water content increases or decreases the rate of diesel infiltration for fine sand and silty clay loams.

Future work for surfactant flushing includes the interfacial change of the biodegradable non-ionic ethoxylated octylphenolic surfactant for diesel and changes of biodegradation rates after surfactant flushing (Cole, 1994; Brusseau et al., 1995; Pope and Wade, 1995; Rouse et al., 1995; Martel et al., 1996). A database could be added of the surfactant brand, surfactant type, and how much it lowers interfacial tension of hydrocarbons and fuels based on composition and mixture. Biodegradation rates of diesel after surfactant flushing using a biodegradable non-ionic ethoxylated octylphenolic surfactant would also be possible future work to determine how much the surfactant may affect bioremediation.

CHAPTER VIII

CONCLUSION

An unfortunate spill of 2000 gallons (7571 liters) of diesel fuel into a fractured karstic dolomite aquifer impacted a municipal water supply well and provided a unique opportunity for field evaluation of analytical LNAPL mass recovery models. This work utilized the opportunity to investigate the accuracy and reliability of nine analytical mass removal models compared to field recovery data. As the aquifer was fully remediated in under two years, the controls on source and removal of diesel mass provides one of the best-controlled field datasets in this type of aquifer. This allowed not only to test the models, but also to evaluate uncertainties in the models to improve estimates of mass recovery in other complex aquifers.

The impacted well site was characterized with electrical resistivity imaging followed by monitoring wells to characterize a perched aquifer and the regional water table. Field methods for removal of diesel in the fractured karst aquifer were documented and overseen by site consultants, various state agencies, and municipal officials to provide accurate removal data for diesel mass. Nine total mechanisms for mass removal occurred to eliminate diesel from the subsurface, with several active methods and some natural mass removal mechanisms. Analytical model methods consisted of either using data from the field site or literature values for either natural or induced methods. Model parameters were selected for minimum, average, and maximum parameters that were observed in the field at the site or other sites from the literature. Modeled values for mass removal were compared to field data for mass removal or with values of remnant mass, as the initial source term was well known.

Results were accurate for several models. Accurate models included evaporation, soil vapor extraction, volatilization, and bioremediation models. Models that over predicted mass removal included excavation, post-surfactant skimmer pump-and-treat and soil vapor extraction models. Models that under predicted included submersible pump-and-treat and pre-surfactant skimmer pump-and-treat. While many of the analytical models were not accurate, they were correct in relative order of magnitudes of removal, predicting which methods would be most effective at removing the majority of the mass.

Uncertainties of the models were contributed by parameter variability and the model variability. Diesel parameters vary based on multiple factors in crude oil origin, distillation method, additives, and company. These free product source parameters for transport are commonly not measured as diesel or other fuels variability is not often considered for mass removal calculations. The variability in the possible values cause significant changes in predicted mass removal. Model variability relies on conceptual model assumptions, simplicity, and unknown parameters changes with the application of surfactants. Surfactant variability in parameters occurs in what mixture is originally utilized and how it interacts with the fuel and matrix. Overall, the models performed adequately in predicting the removal of diesel from the subsurface. In a porous matrix, the models should perform well while in a fractured system, a few modifications may need to be applied. With the use of surfactants, more studies are needed or the development of a separate model to assist in predicting diesel removal in the subsurface.

Future work includes field-testing of diesel fuel parameters from source and free product impact zones to evaluate changes in parameters and the best field method for obtaining the correct transport parameters. The work also demonstrates possible solutions to the uncertainties of the

selected analytical models. Some of the uncertainties for the analytical models could be reduced by adding additional calculations such as infiltration, modeling saturation in a dual porosity matrix, or clarifying assumptions such as how much water moves in a deep well toward the pump, or the assumptions described by Johnson et al., (1990). Further studies of the effects of non-ionic biodegradable surfactants on diesel would better parameterize these reactions for improved modeling. Knowing diesel parameters would reduce the error of several models for diesel mass removal.

REFERENCES

Adamski, M., Kremesec, V., Kolhatkar, R., Pearson, C., and Rowan, B., (2005). "LNAPL in fine-grained soils: Conceptualization of saturation, distribution, recovery, and their modeling." Groundwater Monitoring & Remediation **25**(1): 100-112.

Agency for Toxic Substances and Disease Registry (ATSDR), (1996). Toxicological profile for fuel Oils. Atlanta, GA: U. S. Department of Health and Human Services, Public Health Service.

American Public Health Association (APHA), American Water Works Association (AWWA), and Water Environment Federation (WEF), (1998). Standard Methods for the Examination of Water and Wastewater 20th Edition. United Book Press, Inc., Baltimore, Maryland.

Anderson, W. C. (1993). Innovative site remediation technology: bioremediation, Amer Academy of Environmental.

Anderson, W. C. (1994). Innovative site remediation technology: vacuum vapor extraction, Amer Academy of Environmental.

Atkins, P. W. (2018, 2018/8/7/). "Evaporation." from https://www.accessscience.com:443/content/evaporation/247100.

Barnes, D., Laderach, S. R., and Showers, C., (2002). "Treatment of petroleum-contaminated soil in cold, wet, remote regions." Missoula: USDA Forest Service.

Baú, D. A. and A. S. Mayer (2008). "Optimal design of pump-and-treat systems under uncertain hydraulic conductivity and plume distribution." Journal of contaminant hydrology **100**(1-2): 30-46.

Bogard, V. A. (1973). Soil survey of Pontotoc County, Oklahoma. Washington, Washington U.S. Soil Conservation Service, in cooperation with Oklahoma Agricultural Experiment Station; for sale by the Supt. of Docs., U.S. Govt. Print. Off.

Brock, F. V., Crawford, K. C., Elliott, R. L., Cuperus, G. W., Stadler, S. J., Johnson, H. L., and Eilts, M. D., (1995). "The Oklahoma Mesonet: a technical overview." Journal of Atmospheric and Oceanic Technology **12**(1): 5-19.

Brusseau, M. L., Miller, R. M., Zhang, Y., Wang, X., and Bai, G.-Y., (1995). Biosurfactant-and cosolvent-enhanced remediation of contaminated media, ACS Publications.

Burden, D. S., and National Risk Management Research Laboratory. (2008). A Systematic Approach for Evaluation of Capture Zones at Pump and Treat Systems. U. S. E. P. Agency. Washington, DC, Office of Research and Development.

Calabrese, E. J. and P. T. Kostecki (1991). Hydrocarbon contaminated soils. 5th Conference on Hydrocarbon Contaminated Soils, School of Public Health, University of Massachusetts at Amherst (USA), 1990, Lewis Publishers.

Calabrese, E. J. and P. T. Kostecki (1992). Contaminated soils: diesel fuel contamination, CRC Press.

Chao, H.-P., Lee, J.-F., Juang, L.-C., Kuo, C.-H., and Annadurai, G., (2006). "Volatile organic compounds emission from contaminated soil during surfactant washing." Environmental engineering science **23**(6): 923-932.

Chao, H.-P., Lee, J.-F., Lee, C.-K., Huang, F.-C., and Annadurai, G., (2008). "Volatilization reduction of monoaromatic compounds in nonionic surfactant solutions." Chemical Engineering Journal **142**(2): 161-167.

Charbeneau, R. (2003). "Models for design of free-product recovery systems for petroleum hydrocarbon liquids." American Petroleum Institute. www. api. org/lnapl.

Charbeneau, R. (2007). "LNAPL Distribution and Recovery Model (LDRM) Volume 1: Distribution and Recovery of Petroleum Hydrocarbon Liquids in Porous Media." American Petroleum Institute API Publication **4760**.

Chevalier, L. R. and J. Petersen (1999). "Literature review of 2-D laboratory experiments in NAPL flow, transport, and remediation." Journal of soil contamination **8**(1): 149-167.

Chiu, H., Hong, A., Lin, S. L., Surampalli, R. Y., and Kao, C. M., (2013). "Application of natural attenuation for the control of petroleum hydrocarbon plume: mechanisms and effectiveness evaluation." Journal of hydrology **505**: 126-137.

Christenson, S., Osborn, N. I., Neel, C. R., Faith, J. R., Blome, C. D., Puckette, J., and Pantea, M. P., (2011). Hydrogeology and simulation of groundwater flow in the Arbuckle-Simpson aquifer, south-central Oklahoma, U. S. Geological Survey.

Cohen, R. M., Mercer, J. w., Greenwald, R. M., and Beljin, M. S., (1997). Design guidelines for conventional pump-and-treat systems, United States Environmental Protection Agency, Office of Research and Development, Office of Solid Waste and Emergency Response.

Cole, G. M. (2018). Assessment and remediation of petroleum contaminated sites, Routledge.

Dineen, D. (1991). Remediation options for diesel-contaminated soil. Hydrocarbon Contaminated Soils. E. a. K. Calabrese, P.T. United States, Lewis Publishers. **1:** 181-191.Environment Canada ETC Spills Technology Databases, Oil Properties Database. http://www.etc-cte.ec.gc.ca/databases/oilproperties/(accessed 10/04/2017).

Essaid, H. I., Bekins, B. A., Herkefrath, W. N., and Delin, G. N., (2011). "Crude oil at the Bemidji site: 25 years of monitoring, modeling, and understanding." Groundwater **49**(5): 706-726.

Etkin, D. S. (2009). "Analysis of US oil spillage." API Publication **356**.

Fairchild, R. W., Hanson, R. L., and Davis, R. E., (1990). Hydrology of the Arbuckle Mountains area, south-central Oklahoma, Oklahoma Geological Survey.

Fingas, M. F. (2001). The basics of oil spill cleanup. Boca Raton, Fla., Boca Raton, Fla. : Lewis Publishers.

Fingas, M. F. (2013). "Modeling oil and petroleum evaporation." Journal of Petroleum Science Research.

Fogg, P. G. (2017). Carbon Dioxide in non-aqueous solvents at pressures less than 200 kPa, Elsevier.

Geerdink, M., Loosdrecht, M., and Luyben, K., (1996). "Biodegradability of diesel oil." Biodegradation **7**(1): 73-81.

Gerke, H. and M. T. Van Genuchten (1993). "A dual-porosity model for simulating the preferential movement of water and solutes in structured porous media." Water resources research **29**(2): 305-319.

Gordon, L. and R. W. Murray (2014, 2018/8/7/). "Volatilization." from https://www.accessscience.com:443/content/volatilization/735000.

Greystone Environmental Services, I. (2016a). Site Characterization & Remedial Activities of Diesel Spill, City of Ada, Water Well #1.

Greystone Environmental Services, I. (2016b). Update on Site Characterization & Remedial Activities of Diesel Spill, City of Ada, Water Well #1: *Includes Surfactant Flush and Pump Test Information*.

Ham, W. (1973). Regional Geology of the Arbuckle Mountains, Oklahoma. Oklahoma Geological Survey. The GSA. 1973 Annual Meeting, Dallas Texas.

Hess, A, Höhener, P., Hunkeler, D., and Zeyer, J., (1996). "Bioremediation of a diesel fuel contaminated aquifer: simulation studies in laboratory aquifer columns." Journal of contaminant hydrology **23**(4): 329-345.

Höhener, P., Hunkeler, D., Hess, A., Bregnard, T., and Zeyer, J., (1998). "Methodology for the evaluation of engineered in situ bioremediation: lessons from a case study." Journal of Microbiological Methods **32**(2): 179-192.

Johnson, P., Stanley, C. C., Kemblowski, M. W., Byers, D. L., and Colthart, J. D., (1990). "A practical approach to the design, operation, and monitoring of in situ soil-venting systems." Groundwater Monitoring & Remediation **10**(2): 159-178.

Interstate Technology Regulatory Council (2009). Evaluating LNAPL remedial technologies for achieving project goals, Author Washington, DC.

Kang, S.-H. (1993). "Volatilization and bioremediation potential of soil contaminated by petroleum products."

Khalladi, R., Benhabiles, O., Bentahar, F., and Moulai-Mostefa, N., (2009). "Surfactant remediation of diesel fuel polluted soil." Journal of Hazardous Materials **164**(2-3): 1179-1184.

Ko, N.-Y. and K.-K. Lee (2010). "Information effect on remediation design of contaminated aquifers using the pump and treat method." Stochastic environmental research and risk assessment **24**(5): 649-660.

Kroening, S. J., Leung, D. W., Greenfield, L. G., and Galilee, C., (2011) Losses of Diesel Oil by Volatilisation and Effects of Diesel Oil on Seed Germination and Seedling Growth. Environmental Technology, 22:9, 1113-1117, DOI: 10.1080/09593332208618221.

Krummenacher, J. J., West, K. N., and Schmidt, L. D., (2003). "Catalytic partial oxidation of higher hydrocarbons at millisecond contact times: decane, hexadecane, and diesel fuel." Journal of Catalysis **215**(2): 332-343.

Kunz, R. G. (2011). Environmental calculations: A multimedia approach, John Wiley & Sons.

Kuo, J. (2014). Practical design calculations for groundwater and soil remediation, CRC Press.

Lee, D. H., Cody, R. D., and Hoyle, E. L., (2001). "Laboratory evaluation of the use of surfactants for ground water remediation and the potential for recycling them." Groundwater Monitoring & Remediation **21**(1): 49-57.

Lee, M., Kang, H., and Do, W. (2005). "Application of nonionic surfactant-enhanced in situ flushing to a diesel contaminated site." Water research **39**(1): 139-146.

Lidke, D. J. and C. D. Blome (2017). Geologic Map of the Fittstown 7.5'Quadrangle, Pontotoc and Johnston Counties, Oklahoma, US Geological Survey.

Los Angeles LNAPL Workgroup (2015). Final Report for the LA Basin LNAPL Recoverability Study. Torrance, California.

Lyman, W. J., Reehl, W. F., & Rosenblatt, D. H. (1981). *Research and Development of Methods for Estimating Physicochemical Properties of Organic Compounds of Environmental Concern. Part 2* (No. ADL-C-82426-PT-2). LITTLE (ARTHUR D) INC CAMBRIDGE MA.Ma, Y., Zheng, X., Anderson, S. H., Lu, J., and Feng, X., (2014). "Diesel oil volatilization processes affected by selected porous media." Chemosphere **99**: 192-198.

Ma, Y. F., Li, Y. X., Anderson, S. H., Zheng, X. L., Feng, X. D., & Gao, P. L. (2016). Diesel oil infiltration in soils with selected antecedent water content and bulk density. *Journal of Central South University*, 23(8), 1924-1930.Mackay, D. M. and J. A. Cherry (1989). "Groundwater contamination: pump-and-treat remediation." Environmental Science & Technology **23**(6): 630-636.

Manger, E. D. & Geological Survey. (1963) *Porosity and bulk density of sedimentary rocks*. Geological Survey Bulletin: 1144-E. Washington D.C.: U.S. G.P.O.

Martel, R. and P. J. Gelinas (1996). "Surfactant solutions developed for NAPL recovery in contaminated aquifers." Groundwater **34**(1): 143-154.

Mayer, A. S. and Hassanizadeh S. M., (2005). Soil and groundwater contamination: Nonaqueous phase liquids, American Geophysical Union.

McCoy, K., Zimbron, J., Sale, T., and Lyverse, M., (2015). "Measurement of natural losses of LNAPL using CO2 traps." Groundwater **53**(4): 658-667.

McCoy, K. M. (2012). Resolving natural losses of LNAPL using CO_2 traps, Colorado State University. Libraries.

McKinney, D. C. and M.-D. Lin (1996). "Pump-and-treat ground-water remediation system optimization." Journal of Water Resources Planning and Management **122**(2): 128-136.

McPherson, R. A., Fiebrich, C. A., Crawford, K. C., Kilby, J. R., Grimsley, D. L., Martinez, J. E., Basara, J. B., Illston, B. G., Morris, D. A., and Kloesel, K. A., (2007). "Statewide monitoring of the mesoscale environment: A technical update on the Oklahoma Mesonet." Journal of Atmospheric and Oceanic Technology **24**(3): 301-321.

Mercer, J. W. and R. M. Cohen (1990). "A review of immiscible fluids in the subsurface: properties, models, characterization and remediation." Journal of contaminant hydrology **6**(2): 107-163.

Møller, J., Winther, P., Lund, B., Kirkebjerg, K., and Westermann, P. (1996). "Bioventing of diesel oil-contaminated soil: comparison of degradation rates in soil based on actual oil concentration and on respirometric data." Journal of Industrial Microbiology **16**(2): 110-116.

National Academies of Sciences, Engineeringand Medicine (2015). "Characterization, Modeling, Monitoring, and Remediation of Fractured Rock."

Nester, E. W. (1998). Microbiology : a human perspective. Boston, Mass., Boston, Mass. : WCB McGraw-Hill.

Newell, C. J. (1995). Light nonaqueous phase liquids. Ada, Okla.], Ada, Okla. : United States Environmental Protection Agency, Office of Research and Development, Office of Solid Waste and Emergency Response : Superfund Technology Support Center for Ground Water, Robert S. Kerr Environmental Research Laboratory.

Obigbesan, A., Johns, R. T., Lake, L. W., Bermudez, L., Hassan, M. R., and Charbeneau, R. J., (2001). Analytical Solutions for Free-Hydrocarbon Recovery Using Skimmer and Dual-Pump Wells. SPE/EPA/DOE Exploration and Production Environmental Conference, Society of Petroleum Engineers.

Oklahoma Climatological Survey. (2010) The Climate of Pontotoc County. http://climate.ok.gov/index.php/climate/county_climate_by_county/pontotoc. Accessed on Nov. 07, 2017.

Oklahoma Department of Environmental Quality (2012). Land: Diesel and Gasoline Spills. Publications Clearinghouse of the Oklahoma Department of Libraries. (\fact sheets\land\GasDieselSpillGuidance).

Pickens, C. and Halihan T. (2016) Aquifer Testing of Ada Municipal Supply Wells, Fittstown, Oklahoma. In Update on Site Characterization & Remedial Activities of Diesel Spill, City of Ada, Water Well #1: Includes Surfactant Flush and Pump Test Information. ODEQ Incident #141144.

Pope, G. and W. Wade (1995). Lessons from enhanced oil recovery research for surfactant-enhanced aquifer remediation, ACS Publications.

Qu, Z.-h., Zhao, Y.-s. Zhou, R., Yin, X.-d., Wang, B., and Jiao, L.-n. (2013). "Laboratory-scale analysis of transportation and natural attenuation of diesel fuel in aquifer." Environmental earth sciences **68**(6): 1555-1561.

Rahbeh, M. and R. Mohtar (2007). "Application of multiphase transport models to field remediation by air sparging and soil vapor extraction." Journal of Hazardous Materials **143**(1-2): 156-170.

Ramseur, J. L. (2017). Oil spills: background and governance. Library of Congress. Congressional Research Service.

Risher, J. (1995). "Toxicological profile for fuel oils."

Rouse, J. D., Sabatini, D. A., and Harwell, J. H. (1995). Influence of anionic surfactants on bioremediation of hydrocarbons. ACS symposium series (USA).

Roy, R. and C. W. Greer (2000). "Hexadecane mineralization and denitrification in two diesel fuel-contaminated soils." FEMS microbiology ecology **32**(1): 17-23.

Sabatini, D. A., Knox, R. C., and Harwell, J. H., (1995). Surfactant-enhanced subsurface remediation, American Chemical Society Washington, DC.

Schluep, M. (2000). Dissolution, biodegradation and risk in a diesel fuel contaminated aquifer: modeling and laboratory studies, ETH Zurich.

Soil Survey Staff, Natural Resources Conservation Service, United States Department of Agriculture. Web Soil Survey. Available online at the following link: https://websoilsurvey.sc.egov.usda.gov/. Accessed [12/16/2016].

Song, C. (2000). Chemistry of diesel fuels, CRC Press.

Song, H.-G., Wang, X., and Bartha, R. (1990). "Bioremediation potential of terrestrial fuel spills." Applied and Environmental Microbiology **56**(3): 652-656.

Speight, J. G. and K. K. Arjoon (2012). Bioremediation of petroleum and petroleum products, John Wiley & Sons.

Strbak, L. (2000). "In situ flushing with surfactants and cosolvents." National Network of Environmental Studies Fellowship Report for US Environmental Protection Agency, Office of Solid Waste and Emergency Response Technology Innovation Office, Washington, DC.

Testa, S. M. and D. L. Winegardner (1990). "Restoration of petroleum-contaminated aquifers."

Texas Natural Resource Conservation Commission, (2001). “Total Petroleum Hydrocarbons TNRCC Method 1005: Revision 03, June 1, 2001.”

Udem, S. C., Lekwuwa, I. A., and Udem, N. D. (2011). "Effects of drinking diesel-contaminated water on the hematological and serum biochemical parameters of mice." Comparative clinical pathology **20**(1): 19-23.

U. S. EPA. Office of Solid Waste Emergency Response. (1982). Test methods for evaluating solid waste physical/chemical methods. (2nd ed.). Washington, DC: U.S. Environmental Protection Agency, Office of Solid Waste and Emergency Response : [Supt. of Docs., U.S. G.P.O., distributor].

U. S. EPA, (1991). Survey of Materials-Handling Technologies Used at Hazardous Waste Sites. EPA/540/2-91/010, Office of Research and Development, Washington DC.

U.S. EPA, (1996). Pump-and-Treat Ground-Water Remediation: A Guide for Decision Makers and Practitioners. EPA/625/R-95/005, Office of Research and Development, Washington DC, http://www. epa. gov/ORD/WebPubs/pumptreat.

U.S. EPA (1999) Monitored Natural Attenuation of Petroleum Hydrocarbons. EPA/600/F-98/021, Office of Research and Development, Washington DC,

U.S. EPA (2000) Innovative Remediation Technologies: Field-Scale Demonstration Projects in North America, 2nd Edition. Year 2000 Report. EPA 542-B-00-004, Office of Solid Waste and Emergency Response (5102G), www.epa.gov

U.S. EPA (2005) Cost and Performance Report for LNAPL Recovery: Multi-Phase Extraction and Dual-Pump Recovery of LNAPL at the BP Former Amoco Refinery, Sugar Creek, MO. EPA Office of Solid Waste and Emergency Reposne 542-R-05-016. https://www.epa.gov/sites/production/files/2015-04/documents/cpbpsugarcreek.pdf. Accessed July 23, 2018.

U.S. EPA (2006) In Situ Treatment Technologies for Contaminated Soil. Engineering Forum Issue Paper EPA 542/F-06/013. http://nepis.epa.gov/Adobe/PDF/P1000STG.pdf. Accessed March 18, 2018.

U. S. EPA. Office of Solid Waste and Emergency Response (2012). A citizen's guide to excavation of contaminated soil. EPA 542-F-12-007. https://www.epa.gov/sites/production/files/2015-04/documents/a_citizens_guide_to_excavation_of_contaminated_soil.pdf. Accessed March 28, 2018.

U. S. EPA (2018) Semiannual report of UST performance measures mid fiscal year 2018 (October 1, 2017 - March 31, 2018). https://www.epa.gov/sites/production/files/2018-05/documents/ca-18-12.pdf. Accessed June 22, 2018

U.S. Geological Survey, 2016, National Water Information System data available on the World Wide Web (USGS Water Data for the Nation), accessed [September 16, 2016], at URL [http://waterdata.usgs.gov/nwis/].

Waddill, D. W. and J. C. Parker (1997). "Recovery of light, non-aqueous phase liquid from porous media: Laboratory experiments and model validation." Journal of contaminant hydrology **27**(1-2): 127-155.

Wang, S. and C. N. Mulligan (2004). "An evaluation of surfactant foam technology in remediation of contaminated soil." Chemosphere **57**(9): 1079-1089.

Wang, W., et al. (2014). "Effect of precipitation on LNAPL recovery performance: An integration of laboratory and field results." Journal of Petroleum Science and Engineering **116**: 1-7.

Wodzinski, R. S. and M. J. Johnson (1968). "Yields of bacterial cells from hydrocarbons." Applied microbiology **16**(12): 1886-1891.

Woodrow, J. E. and J. N. Seiber (1988). "Vapor-pressure measurement of complex hydrocarbon mixtures by headspace gas chromatography." Journal of Chromatography A **455**: 53-65.

Zheng, X.-l. and B. LI (2004). "Volatilization behaviors of diesel oil from the soils." Journal of environmental sciences **16**(6): 1033-1036.

APPENDICES

ELECTRONIC APPENDENCIES

E1_EVAPORATION I1

E2_EXCAVATION I2

E3_ API LDRM SUBMERSIBLE PUMP-AND-TREAT A1

E4_ API LDRM SKIMMER PUMP-AND-TREAT A2

E5_ SOIL VAPOR EXTRCTION A3

E6_ API LDRM SKIMMER PUMP-AND-TREAT POST-SURFACTANT FLUSH A4

E7_ SOIL VAPOR EXTRACTION POST-SURFACTANT FLUSH A5

E8_ VOLATILZATION NA1

E9_ BIOREMEDIATION NA2

VITA

Cullen Mikael Pickens

Candidate for the Degree of

Master of Geology

Thesis:
A COMPARISON BETWEEN MODEL AND FIELD DIESEL MASS RECOVERY IN DOLOMITE KARST

Major Field: Geology

Biographical: Born in Norman, Oklahoma, December 31, 1991

Education:

Master of Science, Geology, Oklahoma State Univ., Stillwater, OK in 2018.

Bachelor of Science, Geology, Oklahoma State Univ., Stillwater, OK in 2015.

Associates of Science, Geology, Tulsa Community College, Tulsa, OK in 2013.

Experience:

Graduate Teaching Assistant, Boone Pickens School of Geology, Oklahoma State University, August 2015 – May 2017. Responsibilities include: assisting professors with the preparation and presentation of undergraduate courses, grading, and tutoring.

Publications:

Pickens, C. and Halihan, T., 2018. Field evaluation of diesel mass removal in dolomite karst. Oklahoma Groundwater Association Conference and Trade Show, Oklahoma City, OK, January, 2018

Pickens, C. and Halihan, T., 2017. Field evaluation of diesel mass removal in dolomite karst. Geological Society of America National Annual Conference, Seattle, WA, October, 2017.